compared to the EZ-Wt as control. This result was consistent with that in the TE671/CD4 cells stably expressing the EZ-N (Fig. 1B). However, the EZ-N did not significantly affect the R5-tropic JRFL HIV-1 vector transduction efficiency.

Additionally, we analyzed the effects of the EZ-N on transduction activity and syncytium formation of ecotropic MLV Env proteins in rat XC cells (Kubo et al., 2003). These functions of the ecotropic MLV Env proteins were not affected by the EZ-N

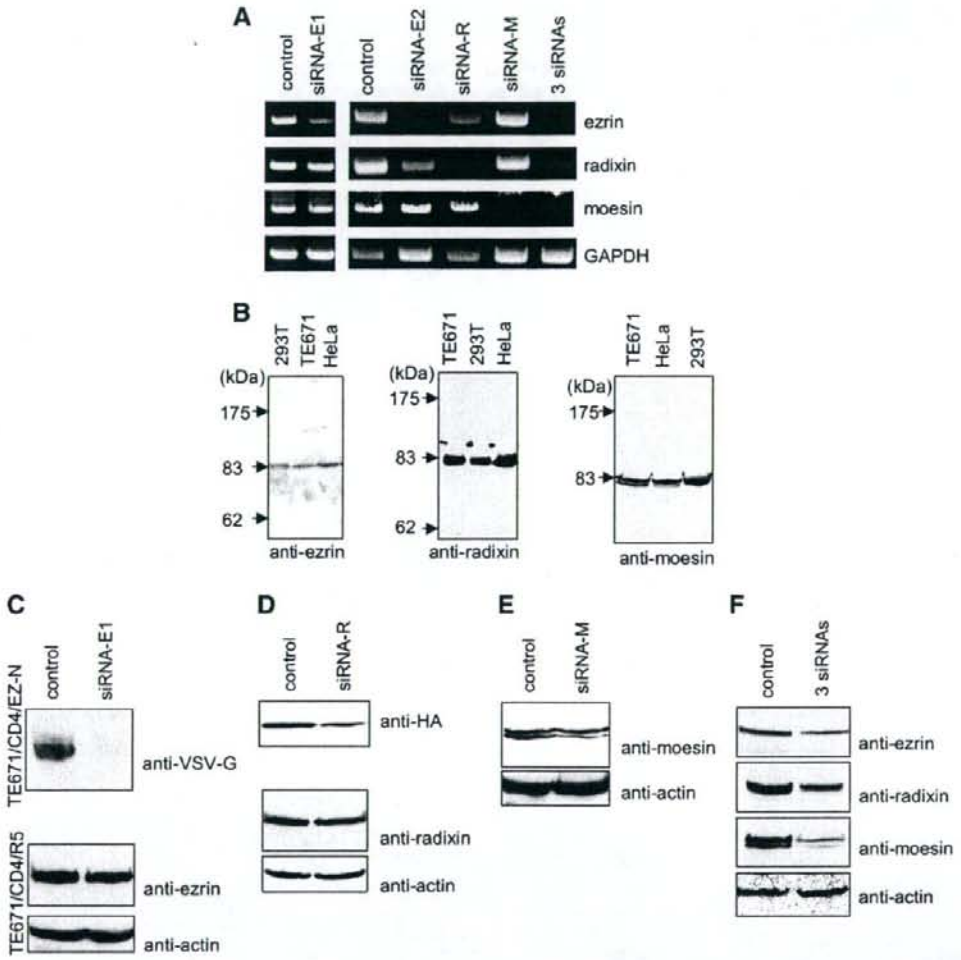

Fig. 3. Knockdown of ERM family proteins by siRNAs. Panel A. Effects of siRNA on ERM mRNA expression. Total RNA samples were isolated from siRNA-GFP-, siRNA-E1-, siRNA-E2-, siRNA-R-, or siRNA-M-transfected TE671/CD4/R5 cells and from cells simultaneously transfected with siRNA-E2, siRNA-R, and siRNA-M (3 siRNAs). Semi-quantitative RT-PCR of these total RNA samples was performed to detect ezrin, radixin, moesin, or GAPDH mRNA. Panel B. ERM family protein expression in human cells. Cell lysates were prepared from 293T, TE671, and HeLa cells, and subjected to Western immunoblotting using the anti-ezrin (left panel), -radixin (middle panel), and -moesin (right panel) antibodies. Molecular size markers are indicated in left side of the panels. Panel C. Effects of siRNA-E1 on ezrin protein expression. Cell lysates were prepared from siRNA-GFP (control)- or siRNA-E1-transfected TE671/CD4 cells expressing the VSV-G-tagged EZ-N mutant. Western immunoblotting of the lysates was performed using the anti-VSV-G epitope antibody. Cell lysates were prepared from siRNA-GFP- or indicated siRNA-E1-transfected TE671/CD4/R5 cells. Western immunoblotting of the lysates was performed using the anti-ezrin or anti-actin antibody. Panel D. Effects of siRNA-R on radixin protein expression. TE671/CD4/R5 cells were transiently transfected with the HA-tagged radixin expression plasmid and an siRNA indicated, and cell lysates were prepared from the transfected cells. Western immunoblotting using the anti-HA antibody was performed. Cell lysates were prepapred from TE671/CD4/R5 cells transfected with the siRNA-GFP or -R. Western immunoblotting using the anti-radixin or anti-actin antibody was performed. Panel E. Effects of siRNA-M on moesin protein expression. Cell lysates were prepared from TE671/CD4/R5 cells transfected with the siRNA-GFP or -M. Western immunoblotting using the anti-moesin or anti-actin antibody was performed. Panel F. Effects of these three siRNAs on ERM protein expression. Cell lysates were prepared from TE671/CD4/R5 cells simultaneously transfected with siRNA-E2, -R, and -R and from cells transfected with siRNA-GFP. Western immunoblotting using anti-ezrin, anti-radixin, anti-moesin, or anti-actin antibody was performed.

expression (data not shown), indicating that ezrin is not associated with the ecotropic MLV Env functions.

Knockdown of ERM family protein expression by siRNA inhibits HIV-1 vector transduction

We were interested in the roles of other ERM family proteins, i.e., radixin and moesin, in HIV-1 infection. siRNAs targeting ezrin, radixin, or moesin mRNA was introduced into the TE671/CD4/R5 cells, and level of the mRNA was monitored by semi-quantitative RT-PCR; siRNA-E1 and -E2 target the ezrin mRNA; siRNA-R targets the radixin mRNA; siRNA-M targets the moesin mRNA. As shown in Fig. 3A, these siRNAs specifically and effectively suppressed expression of corresponding ERM family mRNAs in the TE671/CD4/R5 cells.

We next examined if the siRNAs influence expression levels of the ERM family proteins by Western immunoblotting. As described in manufacture's documents of the antibodies, the commercially available antibodies against the ezrin, radixin, and moesin had strong cross-reactivity due to the high homology within the ERM family proteins. However, we could distinguish moesin from others by the anti-moesin antibody because moesin has smaller molecular size (Fig. 3B, anti-moesin). The moesin was expressed at detectable levels in HeLa and TE671 cells but not in 293T cells. The data with anti-ezrin and anti-radixin antibodies suggest that these proteins were expressed in the three human cells.

To examine siRNA suppression effects on ERM protein expression, we first used anti-VSV-G antibody and examined if exogenous expression of the VSV-G-tagged EZ-N mutant protein in TE671/CD4/EZ-N cells is suppressed by the siRNA against ezrin (siRNA-E1). Target sequence of the siRNA-E1 is located in the N terminal protein-coding region of ezrin mRNA and thus expression of the EZ-N should be suppressed if the siRNA-E1 was functional. Fig. 3C shows that the siRNA-E1 suppressed the expression of the VSV-G-tagged EZ-N mutant protein in TE671/CD4/EZ-N cells, indicating that the siRNA-E1 is functional. As expected, however, we failed to detect the siRNA suppression

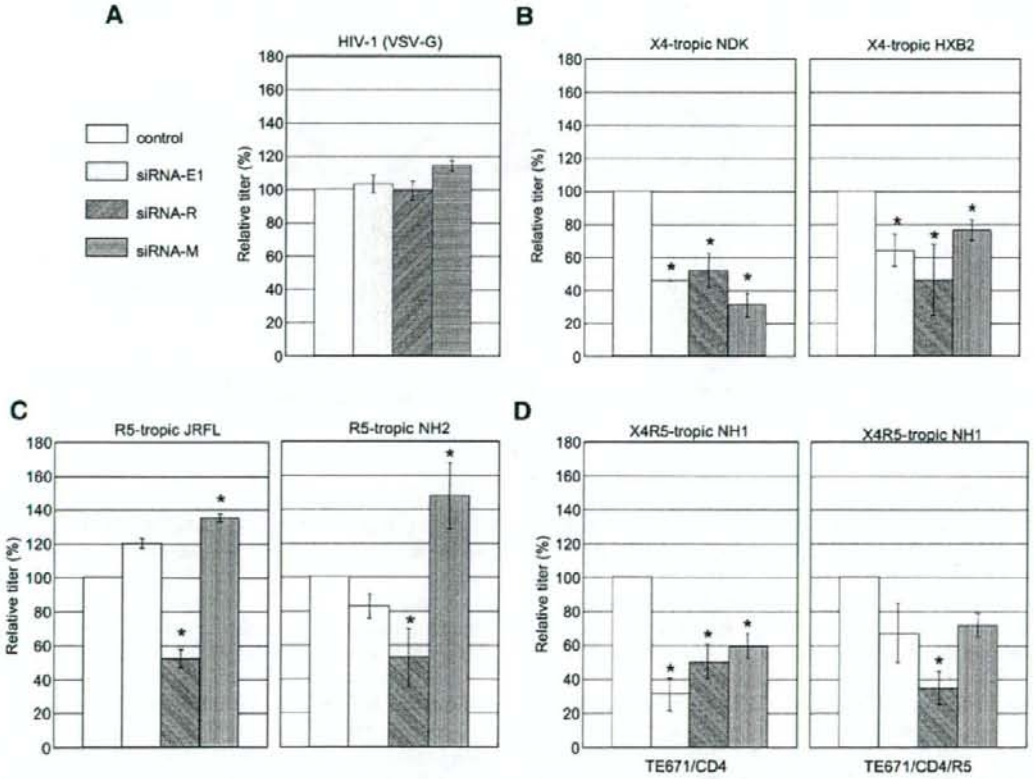

Fig. 4. Effect of siRNAs against ERM family genes on HIV-1 vector transduction. HIV-1 vector pseudotyped with VSV-G (panel A), HIV-1 X4-tropic Env (panel B), or HIV-1 R5-tropic Env (panel C) was inoculated into TE671/CD4/R5 cells transfected with siRNA-GFP, siRNA-E1, siRNA-R, or siRNA-M. HIV-1 vector having the X4R5-tropic NH1 Env protein (panel D) was inoculated into siRNA-transfected TE671/CD4 (left panel) or TE671/CD4/R5 cells (right panel). Relative values to transduction titer in the siRNA-GFP-transfected cells were indicated. This experiment was independently repeated three times. Error bars indicate standard deviations. Asterisks indicate statistical significance ($P<0.05$). Panel E. Cell surface expressions of CD4, CXCR4, and CCR5 in the siRNA-transfected TE671/CD4/R5 cells were analyzed by FACS. Closed areas shows cells stained with the FITC-conjugated secondary antibody alone, and open areas do cells stained with the indicated antibodies and the secondary antibody.

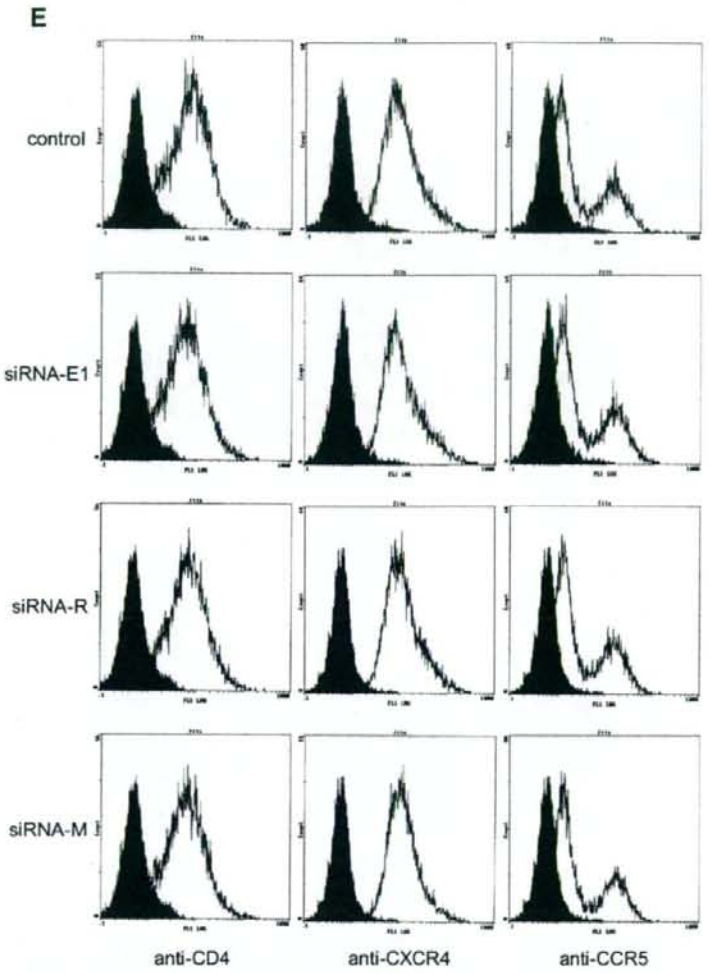

Fig. 4 (*continued*).

effect in the TE671/CD4/R5 cells with the anti-ezrin antibody (Fig. 3C), because the anti-ezrin antibody recognizes radixin as well. Similarly, we failed to confirm suppression of radixin expression by the siRNA-R with the anti-radixin antibody due to the cross-reactivity of the antibody (Fig. 3D). Therefore, we constructed an expression plasmid of a C-terminally HA-tagged radixin (Rad-HA) to confirm whether the siRNA-R is functional. The Rad-HA level in TE671/CD4/R5 cells co-transfected with the Rad-HA expression plasmid and the siRNA-R was lower than that in cells co-transfected with the Rad-HA expression plasmid and the siRNA against GFP (Fig. 3D). In contrast, we could confirm the siRNA-M-mediated suppression of endogenous moesin protein expression with anti-moesin antibody, because molecular size of moesin is smaller than ezrin and radixin (Fig. 3E). When TE671/CD4/R5 cells were simultaneously transfected with the siRNA-E2, -R, and -M, suppressed expression of ezrin, radixin, and moesin proteins was detected using the each antibodies (Fig. 3F). Taken together, our results suggest that these siRNAs inhibit the corresponding protein expression via suppression of mRNA expression.

Transduction titer of the VSV-G vector was not affected by these siRNAs (Fig. 4A), suggesting that VSV-envelope-mediated infection proceeds via ERM-protein independent pathway as already reported (Kameoka et al., 2007). In contrast, transduction titers of the X4-tropic NDK and HXB2 vectors were decreased uniformly by the introduction of siRNA against ezrin, radixin, or moesin (Fig. 4B). X4-tropic transduction efficiency of the X4R5-tropic NH1 vector was also inhibited in TE671/CD4 cells (Fig. 4D), because CC5R is not expressed in the cells. These results were consistent with the data on the ezrin dominant negative mutant (Figs. 1 and 2).

The siRNA-R decreased the titers of the R5-tropic vector and the siRNA-M rather increased the titers (Fig. 4C). These changes were highly reproducible in the repeated experiments.

These effect of the siRNA-mediated knock down of the ERM proteins on the HIV-1 infection was not induced by altered cell surface expression of the HIV-1 receptors, because cell surface expression of the HIV-1 receptors, CD4, CXCR4, and CCR5, were not changed by the siRNAs (Fig. 4E). These results suggest that all of the three ERM family proteins function as positive regulators of the X4-tropic HIV-1 infection, whereas radixin and moesin function positive and negative regulators, respectively, of the R5-tropic HIV-1 infection.

Transduction efficiency of the dual-tropic NH1 vector in TE671/CD4 cells was suppressed by each of the siRNA (Fig. 4D) as that of the X4-tropic vector. Because TE671/CD4 cells do not express CCR5, entry of the dual-tropic NH1 vector occurs only through CXCR4 in the cells. The moesin knockdown in TE671/CD4/R5 cells did not enhance transduction efficiency of the dual-tropic NH1 vector, but did that of the R5-tropic vector. Entry of the NH1 vector was thought to occur through both of CXCR4 and CCR5 in TE671/CD4/R5 cells. Therefore, the effect of moesin knockdown on the dual-tropic vector in TE671/CD4/R5 cells should be different from that on the R5-tropic vector.

To examine if expression of siRNA-resistant ezrin mRNA abrogate the inhibitory effect of ezrin siRNA on the X4-tropic HIV-1 vector transduction, we examined effects of siRNA-E2, which targets 3′ untranslated region (3′UTR) of the ezrin mRNA, on the X4-tropic virus transduction in the TE671/CD4 cells. The siRNA-E2 reduced the endogenous ezrin mRNA level (Fig. 3A), but did not suppress exogenous expression of VSV-G-tagged wild type ezrin (Fig. 5A), because the exogenous mRNA encoding the VSV-G-tagged ezrin does not contain the 3′UTR. The siRNA-E2 transfection into TE671/CD4 cells decreased transduction titer of the NDK HIV-1 vector (Fig. 5B) as the siRNA-E1 did (Fig. 4B). Expression of the siRNA-resistant ezrin, i.e., VSV-G-tagged ezrin wild type protein, abrogated the inhibitory effect of the siRNA-E2 (Fig. 5B). The VSV-G-tagged ezrin expression alone did not affect the HIV-1 vector transduction efficiency. These results support the argument that ezrin is important for increasing efficiency of the X4-tropic HIV-1 infection.

Effects of ERM-family-targeting siRNAs on cell–cell fusion mediated by HIV-1 Env proteins

To assess whether the ERM family proteins play roles in HIV-1-Env-mediated membrane fusion, we examined if the ezrin dominant negative mutant (EZ-N) and siRNAs against the ERM family proteins influence cell–cell fusion in co-culture of target cells and NDK Env-expressing 293T cells. In this co-culture system, we can monitor cell–cell fusion via interaction of HIV-1 Env and HIV-1 infection receptors by using the β-galactosidase activity (see Materials and methods). NDK Env-mediated cell–cell fusion was inhibited by introduction of either the EZ-N protein (Fig. 6A), siRNA-E2, -R, or -M (Fig. 6B) into the receptor expressing cells, consistent with the results obtained from HIV-1 vector transduction assay (Figs. 1B and 4B). Similarly, JRFL-Env-mediated cell–cell fusion was inhibited by ezrin and radixin siRNAs (Fig. 6C), although the ezrin siRNA had no effect on the R5-tropic HIV-1 vector transduction efficiency (Fig. 4C). The siRNA-M enhanced the vector transduction of the R5-tropic vector, whereas such enhancement was not observed in the cell fusion. These effects were highly reproducible in the repeated experiments.

Discussion

In this study, we examined potential roles of the ERM proteins in HIV-1 entry. A recent study described the similar topic, in

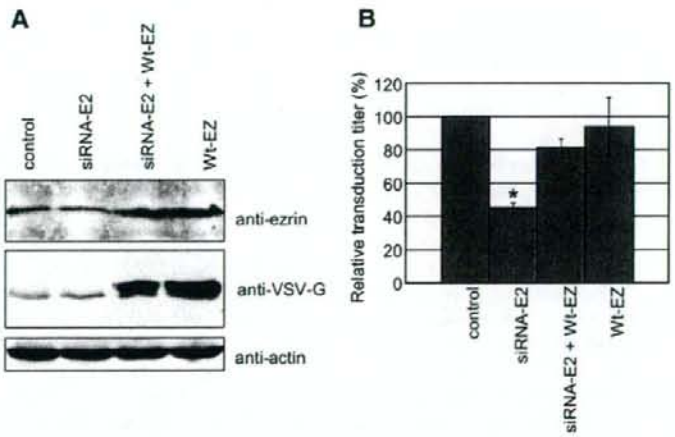

Fig. 5. Abrogation of inhibitory effect of ezrin knockdown on HIV-1 vector transduction by exogenous ezrin expression. Panel A. Cell lystaes were prepared from TE671/CD4/R5 cells transfected with the siRNA-GFP alone, from cells transfected with siRNA-E2 alone, from cells co-transfected with the VSV-G-tagged wild type ezrin expression plasmid and the siRNA-E2, and from cells transfected with the ezrin expression plasmid alone. Westerm immunoblotting of the cell lystaes was performed using the anti-ezrin (upper panel), anti-VSV-G epitope (middle panel), or anti-actin (lower panel) antibody. Panel B. The transfected cells were inoculated with the HIV-1 vector having the NDK Env protein. Relative values to transduction titer in the siRNA-GFP-transfected cells were indicated. This experiment was independently repeated three times. Error bars show standard deviations. Asterisks indicate statistical significance ($P<0.05$).

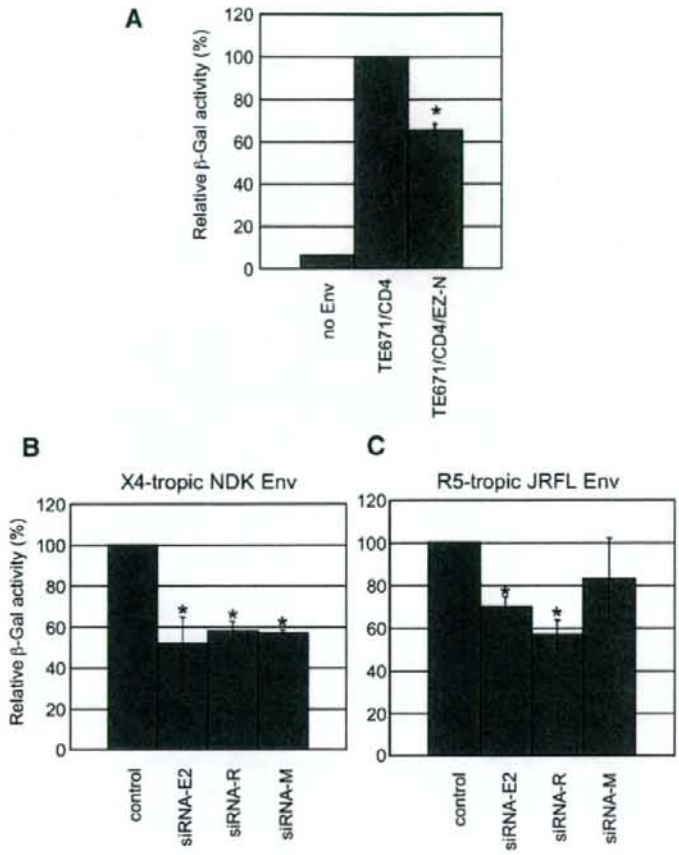

Fig. 6. Effect of ezrin dominant negative mutant and siRNAs against ERM family proteins on HIV-1-Env-mediated cell–cell fusion. 293T cells were transfected with the NDK (panels A and B) or JRFL (panel C) Env expression plasmid. TE671/CD4 or TE671/CD4/EZ-N cells transfected with the LTR-LacZ construct were added onto 293T cells transfected with the NDK Env expression plasmid (panel A). TE671/CD4/R5 cells were co-transfected with the each siRNA as indicated and the LTR-LacZ plasmid. The transfected TE671/CD4/R5 cells were added onto the transfected 293T cells. β-Galactosidase activities of their cell lystaes were measured as described in Materials and methods. Relative values to β-galactosidase activity of the mixed culture of the siRNA-GFP-transfected TE671/CD4/R5 cells and the Env-transfected 293T cells were indicated. This experiment was repeated three times, and error bars indicate standard deviations. Asterisks indicate statistical significance ($P<0.05$).

which the authors showed that the moesin regulates stable microtubule formation and inhibits transduction of HIV-1 vectors having VSV-G protein in the rat cells (Naghavi et al., 2007). Our study deals with the similar topic but rather focused on the roles of the three ERM proteins in HIV-1-Env-mediated infections of human cells rather than VSV-Env-mediated infection of the rodent cells. Our study thus could reveal a hitherto unappreciated regulation mechanism, a pleiotropic regulation of HIV-1 infection by the ERM proteins.

Each of the siRNA against the ERM family proteins as well as the dominant negative mutant of ezrin inhibited transduction of X4-tropic HIV-1 vectors (Figs. 1B and 4B). These inhibitions were unlikely to be due to the reduced binding events of HIV-1 Env to the infection receptors, because the levels of cell surface expression of the CD4 and CXCR4 were similar in the ERM-suppression-positive and -negative cells (Figs. 1C and 4E). Similarly, the inhibitions were unlikely to be due to the overall reductions in the HIV-1 replication processes, because VSV-G-mediated HIV-1 transductions were not affected by the ERM suppression (Figs. 1B and 4A). Alternatively, our results strongly suggest that the ERM suppression induced specific inhibition of the X4-tropic HIV-1 infection at the entry step(s). Correlation between the X4-tropic vector transduction inhibition and cell–cell fusion inhibition (Figs. 4B and 6B) suggests that a key site of action for the siRNA-mediated inhibition is the membrane fusion. This in turn implies that the ERM proteins individually play positive roles in the membrane fusion mediated by interactions of X4-tropic Env and infection receptors.

Interestingly, transductions of the R5-tropic HIV-1 vectors were inhibited by the radixin siRNA alone, but were not by the ezrin and moesin siRNAs (Fig. 4C). The moesin siRNA rather increased the R5-tropic HIV-1 vector transductions. These results suggest that radixin of the ERM family is a key molecule for the efficient R5-tropic HIV-1 infection, whereas moesin rather

suppresses the HIV-1 R5 virus infection. Notably, such bimodal effects of the ERM proteins were not observed in the R5-tropic-Env-mediated cell–cell fusion (Fig. 6C). These results suggest that the ERM proteins including moesin function as positive regulators of R5-tropic-Env-mediated membrane fusion and that moesin additionally functions as a negative regulator of HIV-1 R5 virus replication at the early step(s) after the membrane fusion.

Our findings suggest that the ERM proteins regulate differently the R5- and X4-tropic HIV-1 infection. Underlying mechanisms by which the ERM proteins undergo the different regulation remain to be clarified. In this regard, CCR5 and CD4 co-localize on the plasma membrane before HIV-1 infection (Steffens and Hope, 2003, 2004), whereas CXCR4 and CD4 do not (Kozak et al., 2002). Such a difference in cell surface localization raises a possibility that regulation system for the CCR5 and CXCR4 fluidity on the plasma membrane is different. This in turn may lead to distinct regulation of infection receptor fluidity and cytoskeleton rearrangement by the ERM in CCR5 and CXCR4-mediated HIV-1 infection. However, we cannot exclude the possibility that the CCR5 over-expression in the target cells diminishes the ERM protein function for the R5-tropic HIV-1 infection (Jimenez-Baranda et al., 2007; Viard et al., 2002).

Recent study has reported that the moesin regulates stable microtubule formation and inhibits transduction of HIV-1 vectors having VSV-G protein in the rat cells (Naghavi et al., 2007). The findings suggest that moesin regulates cytoskeleton rearrangement to suppress HIV-1 replication somewhere after virus entry. Our data show that knockdown of moesin by siRNA resulted in enhancement of HIV-1 vector transduction only when the vector has the R5-tropic Env (Fig. 4C). The results suggest that in the case of R5-tropic virus infection, the moesin-mediated enhancement of infection is dominant in comparison with moesin-mediated suppression of HIV-1 replication, if any, after entry. The EZ-N protein suppressed the X4-tropic HIV-1 infection in TE671/CD4 and 293T/CD4 cells, but did not significantly in HeLa/CD4 cells (data not shown). Apparently the inconsistent results with HIV-1 vectors may imply differences of the moesin-mediated regulation system in these different cells, although further study is required for clarifying the issue.

The inhibitory effects of the ezrin dominant negative mutant and the ERM siRNAs on the HIV-1 vector transduction were not so high (about 50% reduction). As mentioned above, ERM proteins are highly homologous each other, and similarly functions, suggesting a possibility that other members of ERM family proteins complement functions of the proteins suppressed by the siRNA. Therefore, the target cells were simultaneously transfected with the siRNAs-E2, -R, and -M. However, the introduction of the three siRNAs resulted in severe cytotoxicity on the target cells as reported (Takeuchi et al., 1994), and it was difficult to analyze their effect on such cells. Transduction titers of the X4-tropic HIV-1 vectors on TE671/CD4 cells transfected with an siRNA against CXCR4, which actually reduced its expression level, was about 50% of those on the GFP siRNA-transfected cells (data not shown), like the ERM siRNAs. This result suggests that the ERM proteins function in X4-tropic HIV-1 entry as importantly as CXCR4 does.

In conclusion, we found that ezrin, radixin, and moesin proteins functions as pleiotropic regulators of HIV-1 infection in human cells. Our findings provide a basis to study HIV-1 entry in relation to the regulation of membrane protein fluidity and cytoskeleton rearrangement by the ERM proteins.

Materials and methods

Env protein expression plasmids

An X4-tropic HIV-1 NDK Env expression plasmid was kindly provided by Dr. U. Hazan (Dumonceaux et al., 1998). HIV-1 HXB2 (X4 tropic), JRFL (R5 tropic), NH1 (X4R5-tropic), and NH2 (R5 tropic) Env expression plasmids were kindly provided by Dr. Y. Yokomaku (Kusagawa et al., 2002; Yokomaku et al., 2004). These HIV-1 Env expression plasmids encodes HIV-1 tat and rev genes as well as the env sequence. A VSV-G expression plasmid (pHEF-VSV-G) was obtained from Dr. L. Chang through the AIDS Research and Reference Reagent Program, Division of AIDS, NIAID, NIH, USA (Iwakuma et al., 1999).

Construction of C-terminally HA-tagged radixin expression plasmid

Total RNA samples were isolated from TE671 cells, and radixin cDNA was amplified by PCR using following primers; Rad-S (5′-GAGAAAGAAAATGCCGAAACC-3′) and Rad-AS (5′-ATATATGCAAAATAACAGCTCTCA-3′). The radixin PCR products were ligated into pTarget vector plasmid (Promega) by TA cloning. The predicted amino acid sequence of the radixin cDNA was completely identical to that of already reported human radixin. The radixin sequence was amplified by PCR using the Rad-S and Rad-HA (5′-TCATGCGTAATCCG-GAACATCGTACGGGTATCCCATTGCTTCAAACTCATC-3′) for C-terminal HA tagging. The antisense Rad-HA primer contains the HA tag sequence. The PCR product was ligated into pTarget vector and its nucleotide sequence was confirmed.

HIV-1 vector

A DNA construct (R8.91) that encodes HIV-1 proteins required for HIV-1 vector preparation except for Env protein was kindly provided by Dr. D. Trono (Naldini et al., 1996). A LacZ-containing HIV-1 vector genome expression plasmid (pTY-EFnLacZ) was obtained from Dr. L. Chang through the AIDS Research and Reference Reagent Program, Division of AIDS, NIAID, NIH, USA (Chang et al., 1999).

Cells

Human TE671, 293T, HeLa cell lines were cultured at 37 C under 5% CO_2 in Dulbecco's modified Eagle's medium (Wako) supplemented with 8% fetal bovine serum (Biosource). CD4-expressing TE671 and HeLa cells (TE671/CD4 and HeLa/CD4) were constructed by transfection with a CD4-expression plasmid containing the neomycin resistant gene. CD4-expressing 293T cells (293T/CD4) were constructed by transfection with a CD4-expression plasmid containing the hygromycin resistant gene. TE671 cells expressing CD4 and CCR5 (TE671/CD4/R5) were

constructed as follows. The TE671/CD4 cells were inoculated with a CCR5 and puromycin-resistant gene-encoding murine leukemia virus (MLV) vector constructed as reported (Kubo et al., 2003), and were selected with puromycin. Puromycin-resistant cell pool was used in this study. TE671 and 293T cells expressing CD4 and a C-terminally VSV-G-tagged dominant negative mutant of ezrin (EZ-N) was constructed by inoculation of the TE671/CD4 and 293T/CD4 cells with an EZ-N-encoding MLV vector constructed as reported (Kubo et al., 2003), and designated as TE671/CD4/EZ-N and 293T/CD4/EZ-N. The VSV-G-tagged EZ-N plasmid was kindly provided from Dr. M. Arpin.

Transduction assay

To obtain HIV-1 vector particles, 293T cells (5×10^5) were plated onto a 10-cm dish and cultured for 2 days. The 293T cells were transfected with the R8.91, pTY-EFnLacZ, and one of HIV-1 Env expression plasmids. The transfected 293T cells were washed to remove the transfection complex 24 h after transfection, and continued to be cultured in fresh medium for additional 24 h. Culture supernatants of the transfected cells were diluted to make their titer about 60 blue-cell-forming units per a microscopic field in ezrin dominant negative mutant-free or siRNA-free cells, and were inoculated into target cells. Target cells (2×10^5) were plated onto a 6-cm dish and were inoculated 24 h after the plating. The inoculated cells were stained with 5-bromo-4-chloro-3-indolyl-β-D-galactopyranoside (X-Gal) (Wako) 2 days after inoculation. Numbers of blue cells were counted to estimate transduction titers.

Western immunoblotting

Cell lysates were subjected to sodium dodecyl sulfate polyacrylamide gel electrophoresis (BioRad), and were transferred onto a PVDF membrane (Millipore). The membrane was treated with an anti-VSV-G (Sigma), -ezrin, -radixin, -moesin, or -actin antibody (Santa Cruz), and then with a horseradish peroxidase-conjugated protein G (BioRad). Protein G-bound polypeptides were visualized by ECL Western blotting detection reagents (Amersham Pharmacia Biotech).

FACS

To analyze cell surface expression of CXCR4 and CCR5, suspended cells were treated with a rat anti-CXCR4 or -CCR5 antibody (Tanaka et al., 2001). The cells were washed with PBS 3 times, and then treated with an FITC-conjugated anti-rat IgG antibody (Sigma). The cells were applied to a flow cytometer (Coulter). To analyze CD4 cell surface expression, cells were treated with an FITC-conjugated anti-CD4 antibody (Sigma).

Transfection of siRNA

Sequences of sense strands of two siRNAs against ezrin were GAAUCCUUAGCGAUGAGAUCU (siRNA-E1) and CCUGAUUCUCGCGAUUAUUCU (siRNA-E2). Sequences of sense strands of siRNAs against radixin and moesin were CGACAAGUUAACACCUAAAU (siRNA-R) and CUCCCAGACGGAUCUGUUGC (siRNA-M). An siRNA against green fluorescence protein (GFP) was used as control, and sequence of the sense strand was CUGGAGUUGUCCCAAUUCUUG. These siRNAs were synthesized by RNAi Co. LTD. Cells were transfected with one of these siRNAs (200 pmol) by the TransIT TKO reagent (10 μl) (Mirus). To knockdown expression of all three ERM family proteins simultaneously, cells were co-transfected with three siRNAs (total 600 pmol) by the transfection reagent (30 μl).

Semi-quantitative RT-PCR

Total RNA was isolated from siRNA-transfected cells. First strand cDNA was synthesized from the total RNA with ramdom hexamer by a reverse transcriptase (TAKARA). Semi-quantitative PCR was performed using the first strand cDNA as template to detect ezrin, radixin, moesin, and GAPDH mRNAs. Nucleotide sequences of the PCR primers for ezrin mRNA were GCACAAACTTACCAG and TGGTCCTGGCCTGGCTGTTA, for radixin mRNA were GGCAACACAAAGCTTTTGCAG and ATATATGCAAAATAACAGCTCTCA, for moesin mRNA were TGAGGCTGTGGAGTGGCAGCA and CTAGAGGCTGGGTGCCCATTA, and for GAPDH mRNA were AGGTCGGAGTCAACGGATTTGGT and GTGGGCCATGAGGTCCACCAC. These primers were synthesized by Genenet Co. Ltd.

Cell-fusion assay

Receptor protein-expressing cells (2×10^5) were plasted onto a 6-cm dish and cultured for 2 days. The cells were co-transfected with the siRNA and a β-galactosidase expression plasmid, in which the β-galactosidase gene is under the control of an HIV-1 long terminal repeat (LTR-LacZ), by the TransIT TKO transfection reagent (Mirus). 293T cells (2×10^5) were plated onto a 6-cm dish and cultured for 2 days. The cells were transfected with a Tat expression plasmid as control or the HIV-1 Env expression plasmid by the Lipofectamine transfection reagent (Invitrogen). The Env expression plmasids additionally encodes the tat gene. The transfected recipient cells (5×10^5) were added onto the HIV-1 Env-expressing 293T cells 24 h after transfection. If these cells fuse, the Tat protein activates the β-galactosidase expression. β-Galactosidase activity of cell lysates was measured 24 h after mixed culture by the high sensitive β-galactosidase activity kit (Stratagene).

Statistical analysis

Differences between two groups of data were determined by the Student's *t*-test. Statistical significance was set at $P<0.05$ for all tests.

Acknowledgments

We thank Dr. U. Hazan for the NDK Env expression plasmid, Dr. Y. Yokomaku for the HXB2, JRFL, NH1, and NH2 Env expression plasmids, Dr. D. Trono for the R8.91 plasmid, Dr. L. Chang for the VSV-G expression plasmid and pTY-EFnLacZ,

and Dr. M. Arpin for the expression plasmids of the wild type and dominant negative forms of ezrin. The VSV-G, TAT, and LacZ-containing HIV-1 vector genome expression plasmids were onbatined through AIDS Research and Reference Reagent Program, NIAID, NIH, USA. This study was supported by a Health Science Research Grant from the Ministry of Health, Labour, and Welfare of Japan and by the 21st century Centers of Excellence (COE) program.

References

Algrain, M., Turunen, O., Vaheri, A., Louvard, D., Arpin, M., 1993. Ezrin contains cytoskeleton and membrane binding domains accounting for its proposed role as a membrane-cytoskeletal linker. J. Cell Biol. 120 (1), 129–139.

Chang, L.J., Urlacher, V., Iwakuma, T., Cui, Y., Zucali, J., 1999. Efficacy and safety analyses of a recombinant human immunodeficiency virus type 1 derived vector system. Gene Ther. 6 (5), 715–728.

Das, V., Nal, B., Roumier, A., Meas-Yedid, V., Zimmer, C., Olivo-Marin, J.C., Roux, P., Ferrier, P., Dautry-Varsat, A., Alcover, A., 2002. Membrane-cytoskeleton interactions during the formation of the immunological synapse and subsequent T-cell activation. Immunol. Rev. 189, 123–135.

Doi, Y., Itoh, M., Yonemura, S., Ishihara, S., Takano, H., Noda, T., Tsukita, S., 1999. Normal development of mice and unimpaired cell adhesion/cell motility/actin-based cytoskeleton without compensatory up-regulation of ezrin or radixin in moesin gene knockout. J. Biol. Chem. 274 (4), 2315–2321.

Dumonceaux, J., Nisole, S., Chanel, C., Quivet, L., Amara, A., Baleux, F., Briand, P., Hazan, U., 1998. Spontaneous mutations in the env gene of the human immunodeficiency virus type 1 NDK isolate are associated with a CD4-independent entry phenotype. J. Virol. 72 (1), 512–519.

Faure, S., Salazar-Fontana, L.I., Semichon, M., Tybulewicz, V.L., Bismuth, G., Trautmann, A., Germain, R.N., Delon, J., 2004. ERM proteins regulate cytoskeleton relaxation promoting T cell-APC conjugation. Nat. Immunol. 5 (3), 272–279.

Fievet, B., Louvard, D., Arpin, M., 2006. ERM proteins in epithelial cell organization and functions. Biochim. Biophys. Acta.

Gupta, N., Wollscheid, B., Watts, J.D., Scheer, B., Aebersold, R., DeFranco, A.L., 2006. Quantitative proteomic analysis of B cell lipid rafts reveals that ezrin regulates antigen receptor-mediated lipid raft dynamics. Nat. Immunol. 7 (6), 625–633.

Iwakuma, T., Cui, Y., Chang, L.J., 1999. Self-inactivating lentiviral vectors with U3 and U5 modifications. Virology 261 (1), 120–132.

Iyengar, S., Hildreth, J.E., Schwartz, D.H., 1998. Actin-dependent receptor colocalization required for human immunodeficiency virus entry into host cells. J. Virol. 72 (6), 5251–5255.

Jimenez-Baranda, S., Gomez-Mouton, C., Rojas, A., Martinez-Prats, L., Mira, E., Ana Lacalle, R., Valencia, A., Dimitrov, D.S., Viola, A., Delgado, R., Martinez, A.C., Manes, S., 2007. Filamin-A regulates actin-dependent clustering of HIV receptors. Nat. Cell Biol. 9 (7), 838–846.

Jolly, C., Kashefi, K., Hollinshead, M., Sattentau, Q.J., 2004. HIV-1 cell to cell transfer across an Env-induced, actin-dependent synapse. J. Exp. Med. 199 (2), 283–293.

Jolly, C., Sattentau, Q.J., 2005. Human immunodeficiency virus type 1 virological synapse formation in T cells requires lipid raft integrity. J. Virol. 79 (18), 12088–12094.

Kameoka, M., Kitagawa, Y., Utachee, P., Jinnopat, P., Dhepakson, P., Isarangkura-na-ayuthaya, P., Tokunaga, K., Sato, H., Komano, J., Yamamoto, N., Oguchi, S., Natori, Y., Ikuta, K., 2007. Identification of the suppressive factors for human immunodeficiency virus type-1 replication using the siRNA mini-library directed against host cellular genes. Biochem. Biophys. Res. Commun. 359 (3), 729–734.

Kikuchi, S., Hata, M., Fukumoto, K., Yamane, Y., Matsui, T., Tamura, A., Yonemura, S., Yamagishi, H., Keppler, D., Tsukita, S., Tsukita, S., 2002. Radixin deficiency causes conjugated hyperbilirubinemia with loss of Mrp2 from bile canalicular membranes. Nat. Genet. 31 (3), 320–325.

Kizhatil, K., Albritton, L.M., 1997. Requirements for different components of the host cell cytoskeleton distinguish ecotropic murine leukemia virus entry via endocytosis from entry via surface fusion. J. Virol. 71 (10), 7145–7156.

Kozak, S.L., Heard, J.M., Kabat, D., 2002. Segregation of CD4 and CXCR4 into distinct lipid microdomains in T lymphocytes suggests a mechanism for membrane destabilization by human immunodeficiency virus. J. Virol. 76 (4), 1802–1815.

Kubo, Y., Ishimoto, A., Amanuma, H., 2003. N-Linked glycosylation is required for XC cell-specific syncytium formation by the R peptide-containing envelope protein of ecotropic murine leukemia viruses. J. Virol. 77 (13), 7510–7516.

Kusagawa, S., Sato, H., Tomita, Y., Tatsumi, M., Kato, K., Motomura, K., Yang, R., Takebe, Y., 2002. Isolation and characterization of replication-competent molecular DNA clones of HIV type 1 CRF01_AE with different coreceptor usages. AIDS Res. Hum. Retrovir. 18 (2), 115–122.

Lehmann, M.J., Sherer, N.M., Marks, C.B., Pypaert, M., Mothes, W., 2005. Actin- and myosin-driven movement of viruses along filopodia precedes their entry into cells. J. Cell Biol. 170 (2), 317–325.

Naghavi, M.H., Valente, S., Hatziioannou, T., de Los Santos, K., Wen, Y., Mott, C., Gundersen, G.G., Goff, S.P., 2007. Moesin regulates stable microtubule formation and limits retroviral infection in cultured cells. EMBO J. 26 (1), 41–52.

Naldini, L., Blomer, U., Gallay, P., Ory, D., Mulligan, R., Gage, F.H., Verma, I.M., Trono, D., 1996. In vivo gene delivery and stable transduction of nondividing cells by a lentiviral vector. Science 272 (5259), 263–267.

Nguyen, D.H., Giri, B., Collins, G., Taub, D.D., 2005. Dynamic reorganization of chemokine receptors, cholesterol, lipid rafts, and adhesion molecules to sites of CD4 engagement. Exp. Cell Res. 304 (2), 559–569.

Platt, E.J., Wehrly, K., Kuhmann, S.E., Chesebro, B., Kabat, D., 1998. Effects of CCR5 and CD4 cell surface concentrations on infections by macrophagetropic isolates of human immunodeficiency virus type 1. J. Virol. 72 (4), 2855–2864.

Pontow, S.E., Heyden, N.V., Wei, S., Ratner, L., 2004. Actin cytoskeletal reorganizations and coreceptor-mediated activation of rac during human immunodeficiency virus-induced cell fusion. J. Virol. 78 (13), 7138–7147.

Rana, T.M., 2007. Illuminating the silence: understanding the structure and function of small RNAs. Nat. Rev., Mol. Cell Biol. 8 (1), 23–36.

Roumier, A., Olivo-Marin, J.C., Arpin, M., Michel, F., Martin, M., Mangeat, P., Acuto, O., Dautry-Varsat, A., Alcover, A., 2001. The membrane-microfilament linker ezrin is involved in the formation of the immunological synapse and in T cell activation. Immunity 15 (5), 715–728.

Saotome, I., Curto, M., McClatchey, A.I., 2004. Ezrin is essential for epithelial organization and villus morphogenesis in the developing intestine. Dev. Cell 6 (6), 855–864.

Steffens, C.M., Hope, T.J., 2003. Localization of CD4 and CCR5 in living cells. J. Virol. 77 (8), 4985–4991.

Steffens, C.M., Hope, T.J., 2004. Mobility of the human immunodeficiency virus (HIV) receptor CD4 and coreceptor CCR5 in living cells: implications for HIV fusion and entry events. J. Virol. 78 (17), 9573–9578.

Takeuchi, K., Sato, N., Kasahara, H., Funayama, N., Nagafuchi, A., Yonemura, S., Tsukita, S., Tsukita, S., 1994. Perturbation of cell adhesion and microvilli formation by antisense oligonucleotides to ERM family members. J. Cell Biol. 125 (6), 1371–1384.

Tanaka, R., Yoshida, A., Murakami, T., Baba, E., Lichtenfeld, J., Omori, T., Kimura, T., Tsurutani, N., Fujii, N., Wang, Z.X., Peiper, S.C., Yamamoto, N., Tanaka, Y., 2001. Unique monoclonal antibody recognizing the third extracellular loop of CXCR4 induces lymphocyte agglutination and enhances human immunodeficiency virus type 1-mediated syncytium formation and productive infection. J. Virol. 75 (23), 11534–11543.

Tsukita, S., Yonemura, S., Tsukita, S., 1997. ERM proteins: head-to-tail regulation of actin–plasma membrane interaction. Trends Biochem. Sci. 22 (2), 53–58.

Viard, M., Parolini, I., Sargiacomo, M., Fecchi, K., Ramoni, C., Ablan, S., Ruscetti, F.W., Wang, J.M., Blumenthal, R., 2002. Role of cholesterol in human immunodeficiency virus type 1 envelope protein-mediated fusion with host cells. J. Virol. 76 (22), 11584–11595.

Yokomaku, Y., Miura, H., Tomiyama, H., Kawana-Tachikawa, A., Takiguchi, M., Kojima, A., Nagai, Y., Iwamoto, A., Matsuda, Z., Ariyoshi, K., 2004. Impaired processing and presentation of cytotoxic-T-lymphocyte (CTL) epitopes are major escape mechanisms from CTL immune pressure in human immunodeficiency virus type 1 infection. J. Virol. 78 (3), 1324–1332.

Overexpressed NF-κB–inducing kinase contributes to the tumorigenesis of adult T-cell leukemia and Hodgkin Reed-Sternberg cells

Yasunori Saitoh,[1] Norio Yamamoto,[1] M. Zahidunnabi Dewan,[1] Haruyo Sugimoto,[1] Vicente J. Martinez Bruyn,[1] Yuki Iwasaki,[1] Katsuyoshi Matsubara,[1] Xiaohua Qi,[1] Tatsuya Saitoh,[2] Issei Imoto,[3] Johji Inazawa,[3] Atae Utsunomiya,[4] Toshiki Watanabe,[5] Takao Masuda,[6] Naoki Yamamoto,[1,7] and Shoji Yamaoka[1]

[1]Department of Molecular Virology, Graduate School of Medicine, Tokyo Medical and Dental University, Tokyo; [2]Department of Host Defense, Research Institute for Microbial Diseases, Osaka University, Suita; [3]Department of Molecular Cytogenetics, Medical Research Institute and School of Biomedical Science, Tokyo Medical and Dental University, Tokyo; [4]Department of Hematology, Imamura Bun-in Hospital, Kagoshima; [5]Department of Medical Genome Sciences, Graduate School of Frontier Sciences, University of Tokyo, Tokyo; [6]Department of Immunotherapeutics, Graduate School of Medicine, Tokyo Medical and Dental University, Tokyo; and [7]AIDS Research Center, National Institute of Infectious Diseases, Tokyo, Japan

The nuclear factor-κB (NF-κB) transcription factors play important roles in cancer development by preventing apoptosis and facilitating the tumor cell growth. However, the precise mechanisms by which NF-κB is constitutively activated in specific cancer cells remain largely unknown. In our current study, we now report that NF-κB–inducing kinase (NIK) is overexpressed at the pretranslational level in adult T-cell leukemia (ATL) and Hodgkin Reed-Sternberg cells (H-RS) that do not express viral regulatory proteins. The overexpression of NIK causes cell transformation in rat fibroblasts, which is abolished by a super-repressor form of IκBα. Notably, depletion of NIK in ATL cells by RNA interference reduces the DNA-binding activity of NF-κB and NF-κB–dependent transcriptional activity, and efficiently suppresses tumor growth in NOD/SCID/γc^{null} mice. These results indicate that the deregulated expression of NIK plays a critical role in constitutive NF-κB activation in ATL and H-RS cells, and suggest also that NIK is an attractive molecular target for cancer therapy. (Blood. 2008;111:5118-5129)

Introduction

The nuclear factor-κB (NF-κB) transcription factors are known to regulate the expression of a wide range of genes involved in development, immune responses, apoptosis, and carcinogenesis as dimers of the REL family members, RelA, RelB, c-Rel, p50, and p52.[1] The p50 and p52 proteins are generated by proteasome-mediated processing of their precursors, p105 and p100, respectively. In resting cells, Rel proteins are sequestered in the cytoplasm through their interactions with the ankyrin repeats of the inhibitory proteins IκBα, -β, and -ε, as well as the precursor proteins p105 and p100. On stimulation, signals converge at the multiprotein IκB kinase (IKK) complex, which is composed of 2 catalytic subunits, IKK1/α and IKK2/β, and the scaffolding proteins, NF-κB essential modulator (NEMO, also known as IKKγ) and ELKS.[2] Phosphorylation by the IKK complex of specific serine residues on the IκB or precursor proteins results in their poly-ubiquitination and proteasome-dependent degradation or processing.[2] Released NF-κB then translocates to the nucleus and regulates expression of target genes.

NF-κB signaling pathways are largely classified as either canonical or noncanonical based on the stimuli and targets of the IKK complex.[2] Canonical activation is induced by stimuli, such as tumor necrosis factor-α (TNFα) and interleukin-1β, and involves NEMO- and IKK2/β-dependent phosphorylation and the subsequent degradation of IκB proteins. Noncanonical NF-κB pathways are activated after the stimulation of a range of TNF receptor family members, such as B-cell activating factor belonging to the TNF family (BAFF) receptor, lymphotoxin-β receptor, Fn14 and CD40, and direct NF-κB–inducing kinase (NIK)- and IKK1/α-dependent phosphorylation and subsequent processing of p100, leading to activation of NF-κB complexes containing RelB.[2,3] Of note in this context, the noncanonical pathways operate in a delayed fashion and are sensitive to protein synthesis inhibition.[4,5]

Compared with the mechanisms underlying the transduction of ligand-induced signaling to NF-κB activation, much less is known about how NF-κB is constitutively activated in a variety of cancer cells.[6] Constitutively high NF-κB activity has typically been demonstrated in human hematopoietic cancer cells, including adult T-cell leukemia (ATL), Hodgkin lymphoma, and multiple myeloma cells.[7,8] We have previously reported the aberrant expression of p52 in ATL and Hodgkin Reed-Sternberg (H-RS) cells that do not express viral regulatory proteins, such as Tax of the human T-cell leukemia virus or latent membrane protein 1 of the Epstein-Barr virus.[9,10] In addition, IKK activation in ATL and H-RS cells was found to be sensitive to protein synthesis inhibition.[10,11] These results indicate that the noncanonical pathways of NF-κB activation operate in these cancer cells. Aberrant p52 expression has also been reported in other types of cancer cells, including breast,[12] prostate,[13] pancreas,[14] and colon.[15] However, the actual triggers of noncanonical NF-κB activation in these cancer cells remain largely unknown except for certain multiple myeloma cells that have mutations in the *NIK*, *TRAF3*, and related genes.[16,17]

Submitted September 10, 2007; accepted February 17, 2008. Prepublished online as *Blood* First Edition paper, February 27, 2008; DOI 10.1182/blood-2007-09-110635.

The online version of this article contains a data supplement.

The publication costs of this article were defrayed in part by page charge payment. Therefore, and solely to indicate this fact, this article is hereby marked "advertisement" in accordance with 18 USC section 1734.

NIK is a serine-threonine kinase that is an essential participant in the induction of the IKK1-dependent processing of p100 as well as IκB degradation in response to stimuli, such as CD70, CD40 ligand, and BAFF.[18] It has also been reported previously that the IKK complex is recruited to CD27 in a manner dependent on NIK function. However, the mechanism by which NIK activity is regulated thereafter was unknown until it was recently demonstrated that these stimuli protect basally translated endogenous NIK protein from proteasome-mediated degradation.[19,20] Liao et al reported that the interaction of NIK with TNF receptor–associated factor 3 (TRAF3) is responsible for the rapid degradation of NIK and that noncanonical NF-κB stimuli induce the degradation of TRAF3 and the elevation of NIK expression.[19] In a separate study, Qing et al have demonstrated that noncanonical NF-κB stimuli stabilize the NIK protein but do not modify its RNA expression or protein translation.[20] The findings of these studies explain the delay in triggering the noncanonical pathway and its high sensitivity to protein synthesis inhibition.

Because NIK is a central regulator of the noncanonical pathway of NF-κB activation, we have investigated in our current study how this kinase is regulated in hematopoietic cancer cells, in which IKK is constitutively activated in the absence of viral regulators.

Methods

Cell culture

ED40515(−),[21] ATL-43Tb(−),[22] and TL-Om1[23] are human T-cell leukemia virus type-I (HTLV-I)–infected T-cell lines established from the leukemic cells of ATL patients. The H-RS cell lines, HDLM-2, L428, and L540, were purchased from the German Collection of Micro-organisms and Cell Cultures (Braunschweig, Germany). CEM[24] and Jurkat[25] are HTLV-I–free human T-lymphoblastic leukemia cell lines. A human B-cell line, Romas RG69,[20] was a kind gift from Dr Gutian Xiao (State University of New Jersey, Piscataway, NJ). Primary leukemia cells derived from ATL patients were obtained under informed consent at Imamura Bun-in Hospital and supplied through the Joint Study on Predisposing Factors of ATL Development. The patients were diagnosed with ATL on the basis of clinical and hematologic features and the presence of antibodies to ATL-associated antigens in serum and of the HTLV-I proviral genome in the leukemia cells. Use of peripheral blood lymphocytes from ATL patients for research purposes was approved by the institutional review board of each institute. Peripheral blood mononuclear cells (PBMCs) derived from healthy donors were also obtained under informed consent. PBMCs were isolated from both ATL patients and healthy donors by density gradient separation with Ficoll-Plaque PLUS (Amersham Biosciences, Uppsala, Sweden). Cells were maintained in RPMI 1640 supplemented with 10% fetal bovine serum, 100 U/mL penicillin G, and 100 μg/mL streptomycin sulfate; 5R is a NEMO-deficient subline of the Rat-1 cell line and has been described previously.[26] B5 and h12 are sublines of Rat-1 and 5R, respectively, express the blasticidin deaminase gene under the control of an NF-κB–dependent promoter, and have also been described previously.[26,27] Plat-E packaging cells were described previously.[28] B5, h12, Plat-E, 293T cells, and mouse embryonic fibroblasts were maintained in Dulbecco modified Eagle medium supplemented with 10% fetal bovine serum, 100 U/mL penicillin G, and 100 μg/mL streptomycin sulfate. Anchorage-independent cell growth was examined essentially as described previously.[29] Images were captured using an inverted microscope (IX70, Olympus, Tokyo, Japan) and processed with Openlab 3.0.2 software (Improvision, Coventry, United Kingdom). Cells used in this study were all maintained at 37°C in air containing 5% CO_2.

Virus infection and transfection

Plat-E cells were transfected with pMRX-HA-NIK-ires-puro, pMRX-HA-kd-NIK-ires-puro, or pMRX-HA-ires-puro (EV1) (Document S1, available on the *Blood* website; see the Supplemental Materials link at the top of the online article) using the calcium phosphate precipitation method. Culture supernatants were collected 48 hours after transfection and filtered. B5 and h12 cells were infected for 2 hours in the presence of 10 μg/mL polybrene. Infected cells were then cultured in medium containing 2 μg/mL puromycin, and cell clones were isolated. Rat fibroblasts expressing SR-IκBα or its empty control vector (EV2) were established essentially as described previously.[10] For production of lentiviruses, 293T cells were cotransfected with pCS-puro-Ctli, pCS-puro-NIKi-1, or pCS-puro-NIKi-2 (Document S1) together with the pCMVΔR8.2 packaging construct and pHCMV-VSV-G (kind gifts from Dr I.S.Y. Chen) using FuGENE 6 (Roche Applied Science, Indianapolis, IN). Culture supernatants were collected 48 hours after transfection and filtered. ED40515(−) and ATL-43Tb(−) cells were infected once or twice with 24 hours interval with these lentiviruses for 6 hours in the presence of 10 μg/mL polybrene. At 48 hours after the infection, cells were cultured in medium containing 2 μg/mL puromycin for an additional 48 hours. These infectants were subjected to immunoblotting, electrophoretic mobility shift assay (EMSA), and transient transfection with 2 μg of IgκCona-luc[30] and pEF1-LacZ[26] using DMRIE-C (Invitrogen, Carlsbad, CA) according to the manufacturer's instructions. Assays for luciferase and β-galactosidase were performed 48 hours after transfection by standard methods. Luciferase activity was normalized on the basis of β-galactosidase activity. The growth of lentivirus-infected cells was determined by the trypan blue staining method.

Immunoprecipitation

For the immunoprecipitation of endogenous NIK, approximately 2×10^7 cells were lysed in buffer A (20 mM Tris-HCl, pH7.5, 0.5% Nonidet P-40, 150 mM NaCl supplemented with 1 μg/mL aprotinin, 1 μg/mL leupeptin, 0.57 mM phenylmethanesulphonylfluoride, 10 μM MG132, 10 μM MG115) followed by preclearing with purified rabbit IgG (Cedarlane Laboratories, Hornby, ON) and protein G-Sepharose beads (Pierce Biotechnology, Rockford, IL). After centrifugation at 14000 rpm for 3 minutes, supernatants were subjected to immunoprecipitation with purified nonimmune rabbit IgG or anti-NIK antibody (#4994) (Cell Signaling Technology, Danvers, MA). Immunoprecipitates were washed 3 times with TNT buffer (20 mM Tris-HCl, pH 7.5, 200 mM NaCl, and 1% Triton X-100). Endogenous NIK proteins were detected by immunoblotting with anti-NIK antibody (#4994). For the immunoprecipitation of HA-tagged NIK, 750 μg cell lysates prepared with buffer A was subjected to immunoprecipitation with anti-HA antibody (12CA5, a kind gift from Dr A. Israël, Institut Pasteur Paris, Paris, France). Immunoprecipitates were washed 3 times with TNT buffer. HA-tagged NIK proteins were detected by immunoblotting with anti-NIK antibody. For immunoprecipitation of endogenous IKK1/2, 1500 μg cell lysates prepared with buffer A were subjected to immunoprecipitation with anti-IKK1 monoclonal antibody (B78-1; BD PharMingen, San Diego, CA) or purified mouse IgG2b (MI10-104; Bethyl Laboratories, Montgomery, TX). Immunoprecipitates were washed 3 times with TNT buffer. Expression of endogenous proteins was detected by immunoblotting with antiphospho-IKK1/IKK2 (Ser180/Ser181) (#2681; Cell Signaling Technology), anti-IKK1 (H-744), or anti-IKK2 (H-470; Santa Cruz Biotechnology, Santa Cruz, CA) antibodies.

Quantitative RT-PCR

Total RNA was extracted using Isogen reagents (Nippon Gene, Tokyo, Japan) according to the manufacturer's instructions. Quantitative RT-PCR amplifications were performed with 100 ng total RNA, 0.3 μM of each primer, and 0.25 μM TaqMan probe using an ABI-7700 Sequence Detector (Applied Biosystems, Foster City, CA): reverse transcription was performed at 48°C for 30 minutes. Taq DNA polymerase was activated at 95°C for 10 minutes, followed by 45 amplification cycles of 95°C for 15 seconds, and annealing and extension at 60°C for 1 minute. The *NIK*, *VEGF*, *ICAM-1*, and *MMP-9* mRNA levels were normalized based on the amount of *18S* ribosomal RNA determined simultaneously by the real-time RT-PCR.

Mice and inoculation of cells

NOD/SCID/γc^{null} (NOG)[31] mice were purchased from the Central Institute for Experimental Animals (Kawasaki, Japan). All mice were maintained under specific pathogen-free conditions in the Animal Center of Tokyo Medical and Dental University (Tokyo, Japan). The Ethical Review Committee of the institute approved the experimental protocol. ED40515(−) cells expressing Ctli or NIKi-1 and -2 were washed twice with serum-free RPMI 1640 and resuspended in the same medium. Mice were anesthetized with ether and inoculated subcutaneously in the postauricular region with 5×10^6 cells per mouse, as described previously.[31] We measured tumor size and weight 2 weeks after cell inoculation.

Statistics

Statistical significance was evaluated using a 2-tailed, unpaired Student's *t* test. *P* values less than .05 were considered to be significant.

Results

NIK is aberrantly expressed in both adult T-cell leukemia and Hodgkin Reed-Sternberg cells

The constitutive processing of p100 to p52 in ATL and H-RS cells[9,10] prompted us to examine whether NIK is aberrantly expressed in both established and primary ATL cells. Immunoblotting of whole-cell lysates prepared from ATL or H-RS cells did not show any detectable NIK signal (data not shown); however, when endogenous NIK was immunoprecipitated from approximately 20 million of these cells and subjected to immunoblotting, NIK was specifically detectable in anti-NIK immunoprecipitates from ATL and H-RS cells, but not from control cells, such as CEM and Jurkat (Figure 1A). Previous studies revealed that inhibition of the proteasome function allowed for detection of endogenous NIK in simple whole-cell lysates of B-cell lines.[19,20] Treatment of ED-40515(−) cells with the MG132 proteasome inhibitor for 3 hours before harvesting enabled us to observe robust endogenous NIK expression at the expected position (Figure 1B). Lysates of 293T cells with or without exogenous NIK expression were used as the positive and negative controls, respectively. We next examined the NIK expression levels as well as those of p100 phosphorylated at serine residues 866 and 870 in a panel of ATL, H-RS, and control cells (Figure 1C). No appreciable NIK expression could be observed in control CEM and Jurkat T-cell lines treated with MG132, in which NF-κB is not constitutively activated. Proteasome inhibition induced strong NIK expression in other Tax-negative ATL-derived cell lines, ATL-43Tb(−) and TL-Om1. Proteasome inhibition also strongly augmented NIK expression in H-RS cells, but only weakly so in the control B-cell lines, RG69. These results indicate that the steady-state levels of NIK of the authentic size are elevated in ATL and H-RS cells, and suggest that NIK may be abundantly produced in ATL and H-RS cells, but is rapidly degraded by the proteasome. The levels of NIK expression correlated well with those of phosphorylated p100 (Figure 1C). Moreover, p52 and the phoshorylated form of IκBα were also abundant in ATL and H-RS cell lines, but not in the control T-cell lines (Figure 1C). These results indicate that the overexpression of NIK is closely linked to the downstream events leading to constitutive activation of the canonical and noncanonical NF-κB pathways in ATL and H-RS cells. A previous study suggested that L428 cells express a C-terminally truncated form of IκBα and that the phosphorylated form of this protein was accumulated after treatment of the cells with proteasome inhibitor or dexamethasone.[32,33] In agreement with this, we did not detect IκBα expression with the antibody used in this study, which recognizes the C-terminus of the protein, but detected the phoshorylated form of this IκBα only after treatment with MG132 (data not shown).

We next investigated *NIK* expression at the mRNA level by quantitative PCR (Figure 1D) and found that that *NIK* transcripts were at between 20- and 100-fold higher levels in ATL and H-RS cells, compared with CEM cells. Next, actinomycin D was used to block new mRNA synthesis, so that decay of existing transcripts could be detected. Quantitative PCR analyses revealed that the half-life of *NIK* mRNA was approximately 3 hours both in the ATL and control T cells (Figure 1E). Essentially similar results were obtained with the other cell lines shown in Figure 1D, including H-RS cell lines (data not shown). A previous report has demonstrated that NF-κB is constitutively activated in primary ATL cells in the peripheral blood.[34] We therefore quantified the *NIK* mRNA levels in PBMCs from both healthy donors and ATL patients (Figure 2A), and found that *NIK* mRNA is overexpressed in PBMCs of 15 of 21 ATL patients. Actinomycin D treatment of PBMCs further revealed that *NIK* mRNA was not apparently stabilized in primary ATL cells (Figure 2B). Moreover, fluorescence in situ hybridization studies on primary ATL cells failed to detect amplification or translocation of the *NIK* gene (Figure S1; Table S2). Finally, when PBMCs were cultured for 3 hours in the presence of MG132, NIK protein was detectable in cells from an ATL patient showing abundant *NIK* mRNA expression, but not in those from a healthy donor (Figure 2C).

NIK transforms rat fibroblasts in an NF-κB–dependent manner

To further explore the roles for NIK during cell transformation, we infected the 3T3-like rat fibroblast cell line Rat-1 with a retroviral vector expressing human NIK and examined its oncogenic activity. As expected, cells transduced with this NIK vector exhibited strong NF-κB DNA binding activity within 36 hours (data not shown). Rat-1 cells transduced with a control retrovirus became resistant to the selection marker puromycin approximately 24 hours after infection and continued to proliferate rapidly. In contrast, Rat-1 cells transduced with the NIK expression vector expressed a readily detectable level of NIK, had a transformed morphology, but ceased proliferating and died within 3 to 4 days after becoming resistant to puromycin. Cells that survived 2 weeks of puromycin selection after NIK transduction eventually appeared indistinguishable from those transduced with the control vector and showed no detectable NIK expression or NF-κB DNA binding activity (data not shown).

Based on these observations, we speculate that the retroviral overexpression of NIK is toxic to the cells so that only cells that had lost its expression could emerge from the puromycin-resistant pools. To address this problem, we used B5 and h12 cells carrying an integrated Igκ2bsrH plasmid that confers resistance to the antibiotic blasticidin S when cells are constitutively expressing active NF-κB.[26] B5 cells are derived from Rat-1 cells, and h12 cells are from 5R cells that lack NEMO expression. When the B5 and h12 cells were transduced with the wild-type NIK retroviral expression vector and subjected to selection with both puromycin and blasticidin S, the majority of the resultant cell clones maintained detectable NIK expression (Figure 3A), elevated catalytic activity of IKK (Figure 4), and the initial transformed morphology (Figure 5B). On the other hand, when B5 and h12 cells were transduced with a retrovirus vector expressing a catalytically inactive mutant form of NIK and selected with puromycin alone, the cells successfully

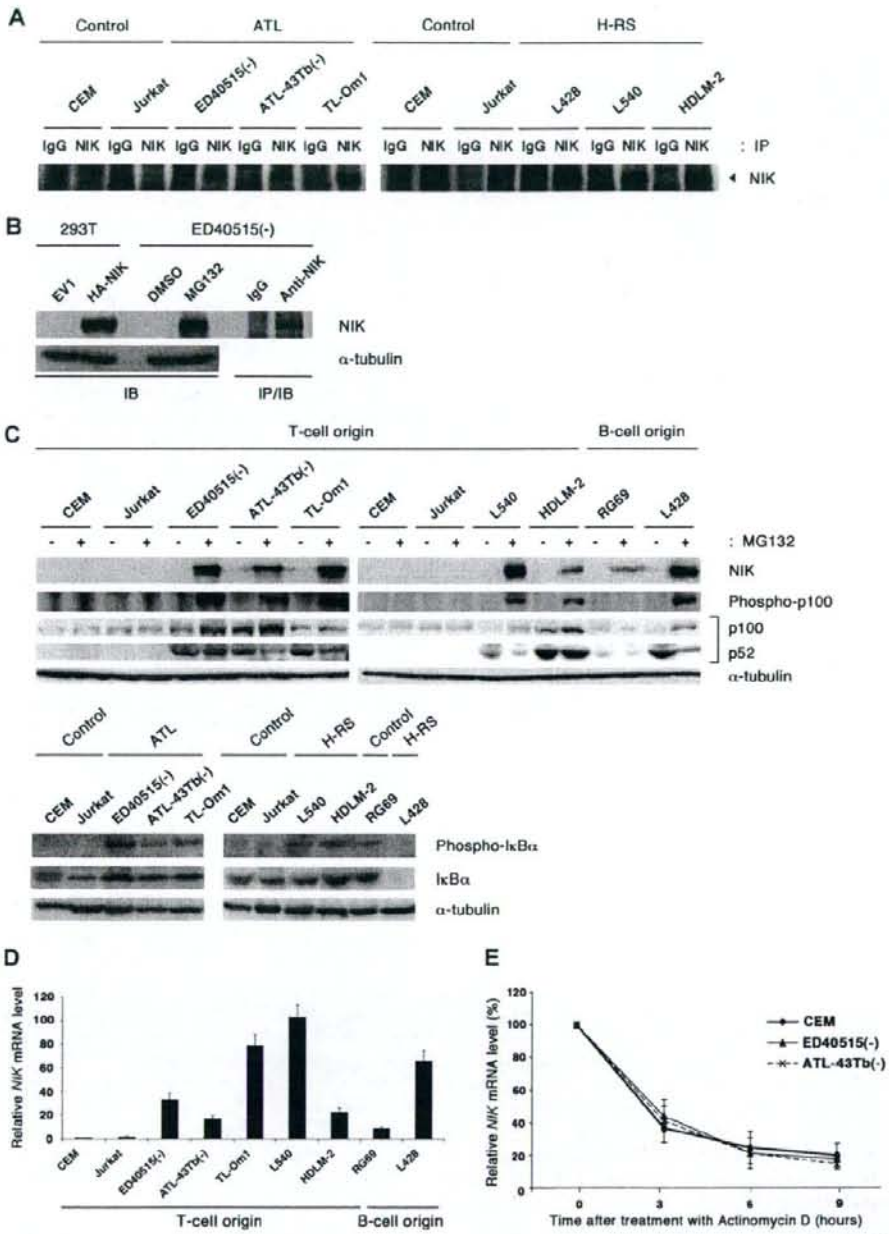

Figure 1. NIK protein is overexpressed in established ATL and Hodgkin Reed-Sternberg cells. (A) Steady-state levels of NIK expression in the ATL and H-RS cell lines were revealed by immunoprecipitation-coupled immunoblotting. Approximately 2×10^7 cells were lysed with buffer A. After preclearing, immunoprecipitation was performed at 4°C, using anti-NIK antibody (NIK) or its isotype IgG (IgG). After 3 washes with TNT buffer, immune complexes were analyzed by immunoblotting with anti-NIK antibody. (B) 293T cells were transfected with pMRX-HA-iresPuro or pMRX-HA-NIKiresPuro for 24 hours. Whole-cell lysates were used as negative and positive controls. ED40515(−) cells were pretreated with (+) or without (−) MG132 (20 μM) for 3 hours, lysed with RIPA buffer, and subjected to immunoblotting with anti-NIK or anti-α-tubulin antibodies. Immunoprecipitation-coupled immunoblotting was performed as in panel A. (C) Top panels: control T-cell lines (CEM and Jurkat), leukemic cell lines derived from ATL patients that do not express Tax (ED40515(−), ATL43-Tb(−), and TL-Om1, a control B-cell line (RG69), and H-RS cell lines (HDLM-2 and L540) were pretreated with (+) or without (−) MG132 (20 μM) for 3 hours, and 30 μg of the whole-cell extracts were subjected to Western blot analysis with the antibodies to the indicated proteins. Bottom panels: Whole-cell extracts from the indicated cell lines were analyzed by Western blotting with the antibodies to the indicated proteins. (D) Total RNA was extracted from the indicated cell lines and subjected to real-time RT-PCR to quantify the *NIK* mRNA levels. The *NIK* mRNA levels were normalized to *18S* RNA. The relative *NIK* mRNA levels shown represent the fold increases in mRNA abundance, relative to that of the CEM cells (arbitrarily set at 1). (E) Cells were cultured in the presence of actinomycin D (5 μg/mL) for the times indicated, and then total RNA was isolated and subjected to quantitative RT-PCR as in panel D. Data are expressed as mean plus or minus SD of 3 independent experiments. The relative amounts of *NIK* mRNA shown represent the percentages in mRNA abundance, relative to that of each cell line before the addition of actinomycin D (arbitrarily set at 100%). IB indicates immunoblotting; IP, immunoprecipitation.

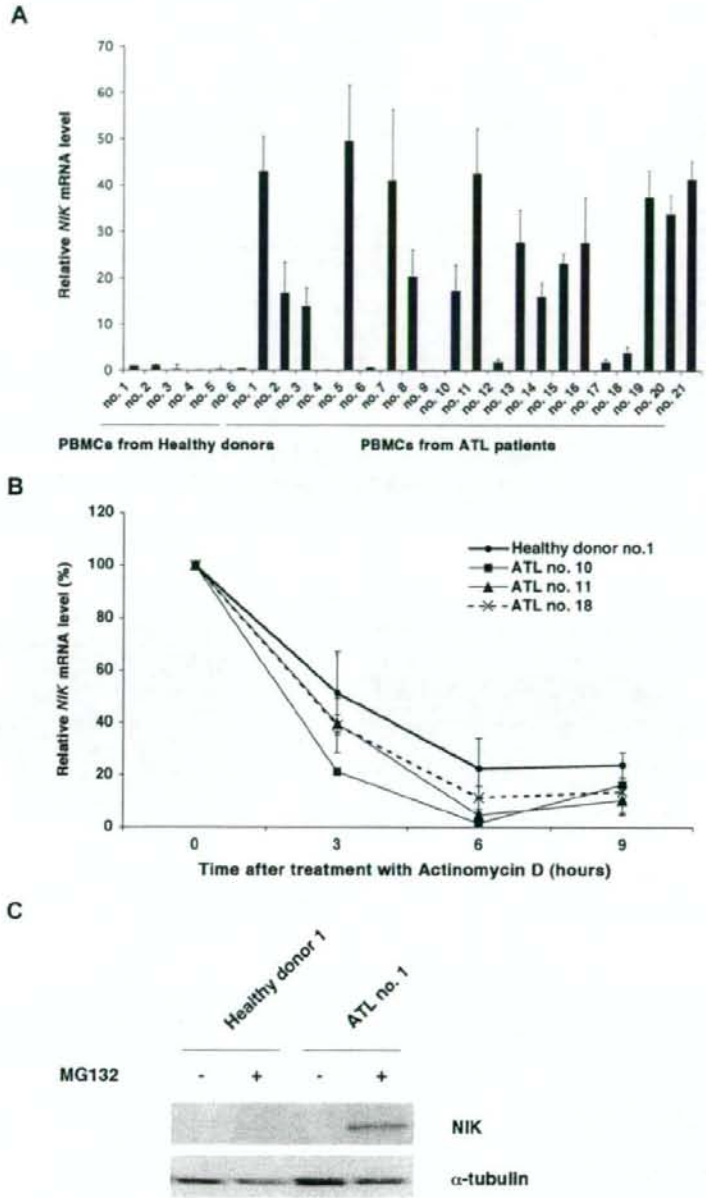

Figure 2. Overexpression of the *NIK* mRNA and protein in PBMCs from ATL patients. (A) Total RNA was extracted from PBMCs from healthy donors and ATL patients and then subjected to quantitative RT-PCR. The *NIK* mRNA levels were normalized to *18S* RNA. The relative *nik* mRNA levels shown represent the fold increases in mRNA abundance relative to that of healthy donor 1 (arbitrarily set at 1). These data are expressed as the mean plus or minus SD of 3 independent experiments. (B) PBMCs were cultured in the presence of actinomycin D (5 μg/mL) for the times indicated, and then total RNA was isolated and subjected to quantitative RT-PCR. The relative amounts of *NIK* mRNA shown represent the percentages in mRNA abundance, relative to that of PBMCs before the addition of actinomycin D (arbitrarily set at 100%). (C) PBMCs from a healthy donor and an ATL patient were treated with (+) or without (−) MG132 (20 μM) for 3 hours, lysed with RIPA buffer, and subjected to immunoblotting with anti-NIK or anti-α-tubulin antibodies.

expressed this protein (Figure 3A) without significant morphologic change (Figure 5B) or constitutive NF-κB activation (Figure 3C). As expected, these cells failed to survive selection with blasticidin S (data not shown).

The expression of wild-type NIK in B5 and h12 cells potently induces p52 expression and NF-κB DNA binding activity, whereas the catalytically inactive NIK mutant does not (Figure 3B,C). We also found a specifically phosphorylated form of IκBα in cells expressing wild-type NIK (Figure 3A). Super-shift experiments revealed that the NF-κB–DNA binding complexes in B5 and h12 cells expressing NIK involve p50, RelB, and RelA (Figure 4D). The presence of p52 in the DNA binding complexes could not be examined, however, because an antibody recognizing rat p52 in super-shift assay is not currently available. Instead, we analyzed DNA-binding complexes induced by NIK expression in wild-type mouse embryonic fibroblasts (Figure S2). Retroviral overexpression of NIK indeed induced DNA-binding NF-κB complexes containing p52, and enhanced expression of p52 and phosphorylated form of IκBα.

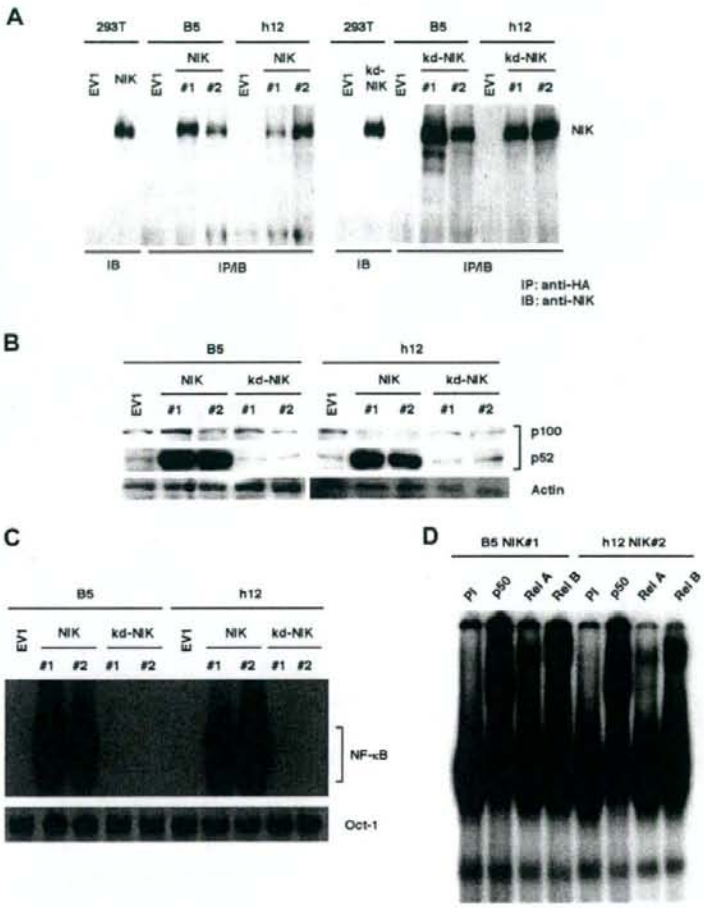

Figure 3. NIK induces constitutive NF-κB activity in rat fibroblasts. (A) B5 and h12 cells were infected with retroviruses capable of expressing HA-tagged NIK (NIK) or catalytically inactive NIK (kd-NIK). Pools of B5 and h12 cells transduced with the control pMRX-HAiresPuro vector (EV1) were used as a control. Cytoplasmic extracts from EV1 and 2 independent cell clones (no. 1 and no. 2) were subjected to immunoprecipitation using antibody against the HA epitope. Immunoprecipitates were then resolved by 8% SDS-PAGE and subjected to immunoblotting with anti-NIK antibody. 293T cells were transiently transfected with the pMRX-HAiresPuro vector (EV1) or pMRX-HA-NIKiresPuro (NIK). Cytoplasmic extracts (30 μg) were then used for immunoblotting as negative and positive controls, respectively. (B) Elevated p52 production in rat fibroblasts. Whole-cell lysates from B5 and h12 cells expressing wild-type NIK or kd-NIK were subjected to SDS-PAGE and immunoblotting with anti-p52 for detection of p100 and p52 or antiactin antibodies. (C) Elevated NF-κB–DNA binding activity in rat fibroblasts. 5 μg of nuclear extracts prepared from B5 and h12 cells expressing wild-type NIK or kd-NIK were analyzed by EMSA, using oligonucleotides encoding an NF-κB–binding sequence or Oct-1–binding sequence as probes. (D) DNA-binding NF-κB components in B5 and h12 cells expressing wild-type NIK were analyzed by super-shift EMSA. Nuclear extracts (5 μg) from B5 NIK#1 and h12 NIK#2 cells were preincubated for 30 minutes with preimmune (PI), anti-p50, anti-RelA or anti-RelB sera, and then subjected to EMSA with the NF-κB–specific probe. IB indicates immunoblotting; IP, immunoprecipitation.

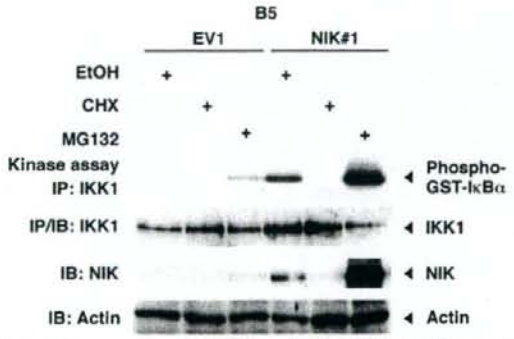

Figure 4. NIK expression parallels IKK activity after CHX or MG132 treatment. B5 cells transduced with the control vector (EV1) or B5 cells expressing wild-type NIK (NIK#1) were treated for 4 hours with either vehicle (ethanol, EtOH), cycloheximide (CHX; 50 μg/mL), or MG132 (20 μM). Cytoplasmic extracts were subjected to immunoprecipitation with IKK1-specific antibody, and then immunoprecipitates were used for an in vitro kinase assay. IKK1 expression in the immunoprecipitates was revealed by immunoblotting with IKK1-specific antibody. NIK and actin levels in the cytoplasmic extracts used for immunoprecipitation were determined by immunoblotting with anti-NIK or antiactin antibodies, respectively. IB indicates immunoblotting; IP, immunoprecipitation; GST, glutathione-S-transferase tag.

We have previously demonstrated that the treatment of ATL cells with MG132 greatly enhances IKK activity, whereas protein synthesis inhibition quickly abolished this activity.[11] Figure 4 shows that the IKK activity in B5 cells stably expressing NIK (NIK#1) is modulated by MG132 and cycloheximide (CHX) in a manner that is very similar to that seen in ATL cells. In addition, treatment of NIK#1 cells with MG132 remarkably elevates the level of exogenous NIK expression. The constitutive NF-κB activation caused by the presence of exogenous NIK was found to be abolished by the retroviral expression of a super-repressor form of IκBα (SR-IκBα), without affecting exogenous NIK expression (Figure 5A). Interestingly, the forced expression of SR-IκBα also diminishes the p52 and p100 expression levels.

We next tested the ability of NIK to induce anchorage-independent growth of rat fibroblasts. B5 and h12 cells transduced with the control vector did not form colonies of significant size in soft agar, whereas those transduced with wild-type NIK expression vector formed a number of large colonies, as shown in Figure 5B and Table 1. Cells expressing catalytically inactive NIK failed to form colonies in soft agar. The expression of SR-IκBα completely abolished NIK-induced colony formation and also the morphologic alterations of B5 and h12 cells. Given that SR-IκBα specifically suppresses NF-κB activation,

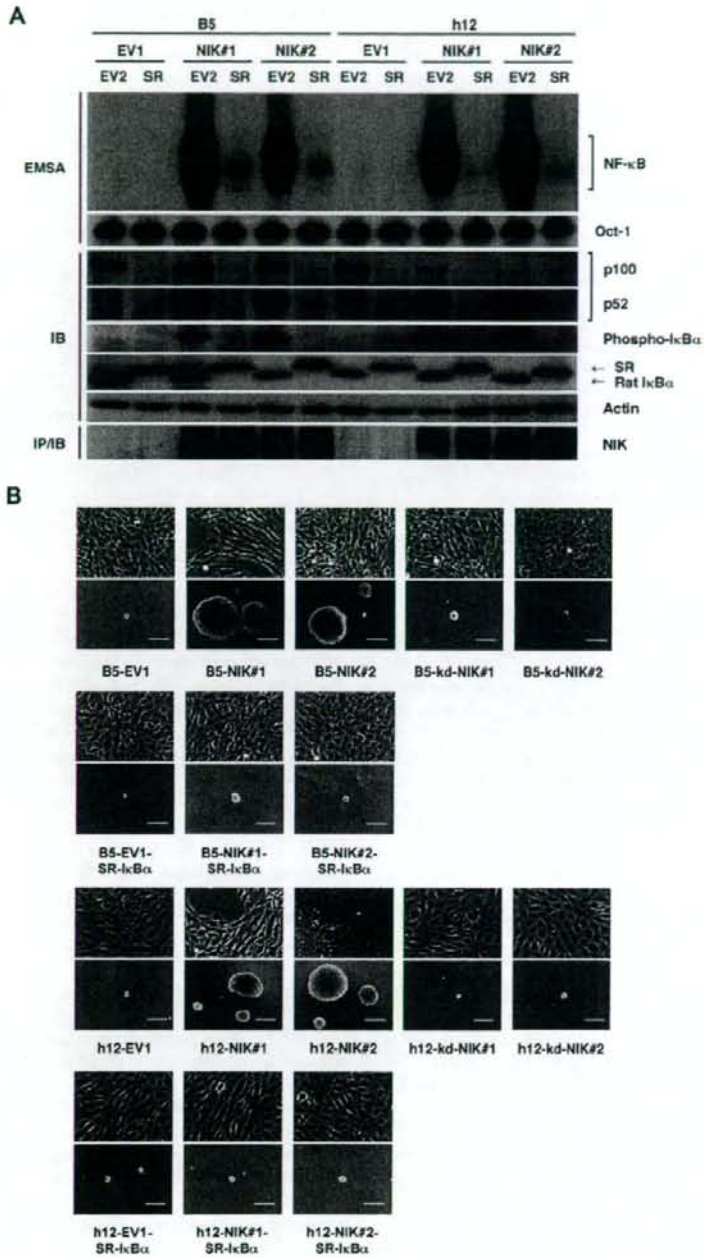

Figure 5. The overexpression of NIK transforms rat fibroblasts in an NF-κB–dependent manner. (A) Top 2 panels: 5 μg of nuclear extracts prepared from B5 and h12 cells transduced with empty vector (EV2) or SR-IκBα (SR) were analyzed by EMSA, using NF-κB and Oct-1 probes. Middle 5 panels: whole-cell extracts (30 μg) of B5 or h12 infectants were subjected to SDS-PAGE and immunoblotting with anti-p52, antiphospho-IκBα, anti-IκBα, or antiactin antibodies. Bottom panel: HA-tagged NIK was immunoprecipitated from B5 and h12 infectants with anti-HA antibody and detected by immunoblotting with anti-NIK antibody (H-248). (B) Phase-contrast micrographs of cells cultured on monolayers (top images) or in soft agar (bottom images). B5 or h12 cell clones expressing wild-type NIK (NIK#1 and NIK#2) or not (EV1) were cultured in soft agar for 3 weeks. These cells were further transduced with SR-IκBα, and then pooled cells were assayed for anchorage-independent growth in soft agar. B5 and h12 cell clones expressing kd-NIK were also examined. Original magnification × 100. Scale bar represents 100 μm. SR indicates super-repressor; kd-NIK, catalytically inactive NIK; IB, immunoblotting; IP, immunoprecipitation.

we conclude from these results that NIK transforms rat fibroblasts in an NF-κB–dependent manner.

NIK mediates constitutive NF-κB activation in ATL cells

The similar modulation of IKK activity by CHX or MG132 in both ATL and B5 cells expressing NIK (Figure 4) suggests that NIK plays an important role in constitutive NF-κB activation in ATL cells. We therefore examined whether the RNA interference-mediated silencing of endogenous *NIK* gene expression would lower NF-κB–dependent transcription in these cells. ED-40515(−) and ATL-43Tb(−) cells were infected with lentiviral constructs that express short hairpin RNA (shRNA) molecules that target mRNA for either *Renilla luciferase* (Ctli) or *NIK* (NIKi), and then subjected to puromycin selection for 2 days. To

Table 1. Efficiency of colony formation in soft agar

Cells*	Colony-forming efficiency, %	Average size of colonies, μm†
B5-EV1	0.7 ± 0.5	62.6 ± 1.5
B5-NIK#1	23.2 ± 2.0‡	236.2 ± 12.6‡
B5-NIK#2	18.9 ± 2.4‡	184.1 ± 19.8‡
B5-kd-NIK#1	1.5 ± 0.3	63.1 ± 1.4
B5-kd-NIK#2	1.3 ± 0.1	62.8 ± 1.8
h12-EV1	1.2 ± 0.3	60.5 ± 0.0
h12-NIK#1	12.8 ± 1.7‡	146.9 ± 4.6‡
h12-NIK#2	17.7 ± 1.7‡	154.9 ± 5.6‡
h12-kd-NIK#1	1.4 ± 1.0	61.5 ± 2.1
h12-kd-NIK#2	1.5 ± 0.4	62.5 ± 4.7
B5-EV1-EV2	1.2 ± 0.3	61.8 ± 1.1
B5-NIK#1-EV2	21.1 ± 1.0‡	193.8 ± 3.7‡
B5-NIK#2-EV2	14.3 ± 1.0‡	150.4 ± 8.7‡
h12-EV1-EV2	1.5 ± 0.7	60.8 ± 0.4
h12-NIK#1-EV2	12.3 ± 1.7‡	119.4 ± 5.6‡
h12-NIK#2-EV2	14.0 ± 1.8‡	160.3 ± 7.2‡
B5-EV1-SR-IκBα	1.5 ± 0.0	61.7 ± 0.5
B5-NIK#1-SR-IκBα	3.4 ± 0.0	64.8 ± 1.1
B5-NIK#2-SR-IκBα	3.9 ± 0.1	63.3 ± 0.4
h12-EV1-SR-IκBα	1.7 ± 1.0	61.3 ± 0.4
h12-NIK#1-SR-IκBα	2.7 ± 0.3	62.3 ± 0.1
h12-NIK#2-SR-IκBα	3.4 ± 1.4	61.4 ± 0.2

kd-NIK indicates catalytically inactive NIK; SR, super-repressor; EV1, empty vector for NIK or kd-NIK; and EV2, empty vector for SR-IκBα.

*Cells were inoculated in 0.33% soft agar and cultured for 3 weeks.

†Colonies larger than 60 μm were counted as positive. The sizes of more than 100 positive colonies were averaged.

‡$P < .05$ vs B5-EV1.

suppress NIK expression maximally, we used independently or in combination 2 shRNAs (NIKi-1 and -2) that target different *NIK* sequences and reduce NIK expression. The infected cells were then assayed for transcriptional activity by transient transfection with an NF-κB–dependent reporter gene (Figure 6A). Lentiviral expression of NIKi constructs resulted in suppression of NF-κB–dependent reporter gene expression in ATL cells when independently used, and the combined use of the 2 NIKi constructs (NIKi-1 and -2) was found to be more effective. We then examined ATL cells transduced with NIKi-1 and -2 constructs for the expression of endogenous NIK and specifically phosphorylated forms of p100, IκBα, and IKKs by immunoblotting (Figure 6B) and for NF-κB DNA binding activity by EMSA (Figure 6C). NIK expression in ATL cells was found to be down-regulated by the shRNA-mediated silencing (Figure 6B). As expected, p52 and phosphorylated p100 were also reduced by NIK depletion, and interestingly, phoshorylation of IκBα was also suppressed. This is consistent with the results observed in NIK-transduced rat fibroblasts that express the phoshorylated form of IκBα (Figure 5A), indicating that NIK, when aberrantly and stably expressed, induces phosphorylation of IκBα. In addition, NIK depletion suppressed phosphorylation of the serine residues in the activation loop of IKKs, suggesting a key role for NIK in constitutive activation of IKKs in ATL cells (Figure 6B). Moreover, depletion of NIK resulted in suppression of NF-κB DNA binding activity (Figure 6C). Super-shift assays revealed that DNA-binding of NF-κB components, p50, p52, RelA, and RelB was reduced by NIK depletion (Figure 6D). As shown previously, c-Rel was not detected in ATL cells.[34] We further investigated alterations in the expression of NF-κB target genes by NIK depletion. Vascular endothelial growth factor (VEGF), matrix metalloproteinase-9 (MMP-9), and intracellular adhesion molecule-1 (ICAM-1), the expression of which has been reported to be under the control of NF-κB,[35-37] are highly expressed in ATL cells and suggested to contribute to their invasive properties.[38-41] Quantitative RT-PCR studies reveal that depletion of NIK results in down-regulation of the expression of these NF-κB target genes (Figure 6E).

NIK regulates tumorigenicity of ATL cells in vivo

We finally investigated biologic effects of NIK depletion in ATL cells. NIK depletion did not significantly influence the growth of cells in culture (Figure 7A). We then examined whether depletion of NIK affects the tumorigenicity of ATL cells in a mouse model. NOD/SCID/γc^{null} mice were subcutaneously inoculated with ED-40515(−) cells that express Ctli or NIKi and are characterized in Figure 6B,C, and tumor formation was evaluated 2 weeks later. As expected, ED-40515(−) cells expressing Ctli efficiently formed large tumors, whereas tumors formed in mice inoculated with ED-40515(−) cells expressing NIKi were significantly smaller (Figure 7B-D), suggesting that NIK supports efficient tumor cell growth in vivo.

Discussion

Persistent activation of NF-κB has previously been reported to play an essential role in the growth and survival of specific cancer cell types, including ATL, H-RS, melanoma, and prostate cancer cells.[9,42-45] Inappropriate NF-κB activation can also contribute to the resistance to the apoptotic responses induced by certain anticancer drugs.[46] On the other hand, cancer cell apoptosis can be induced when persistent NF-κB activity is blocked by inhibitors, such as SR-IκBα, by drugs targeting IKK or the proteasome, via peptides targeting p50 or NEMO, and by double-stranded oligonucleotides containing NF-κB binding sites.[47,48] One problem with such inhibitors, however, is their lack of specificity to cancer cells because they also necessarily block normal NF-κB activation. Hence, it would be desirable to specifically inhibit NF-κB activation in cancer cells by identifying molecular targets in each cancer type. Virally transformed cancer cells express a virus-derived regulatory protein(s) that targets critical molecules in a variety of key signaling pathways. Cytokine autocrine loops or genetic alterations to genes regulating the NF-κB signaling mechanisms that lead to persistent NF-κB activation have also been identified in some cancer cells.[16,17,32,47,49] However, the mechanisms underlying persistent NF-κB activation in many types of cancer remain unknown.

Most primary ATL cells, although infected with HTLV-I, are characterized by the loss of viral protein expression, including Tax, probably because of the host immune surveillance during the long period of latency.[50] Nevertheless, NF-κB is strongly and persistently activated in ATL cells through IKK,[9] although the mechanism of IKK activation has remained unknown. The findings in our present study demonstrate the aberrant expression of *NIK* at the pretranslational level in ATL cells derived from 15 of 21 patients. This overexpression does not seem to correlate with the patients' age, sex, disease type, or percentage of abnormal lymphocytes (Table S1). Further studies will be required to clarify potentially NIK-independent NF-κB activation in the other 6 cases. The stable expression of functional NIK in fibroblasts, but not that of its catalytically inactive mutant, causes cellular transformation and persistent NF-κB activation with molecular features quite similar to those reported previously in ATL cells. These include the rapid

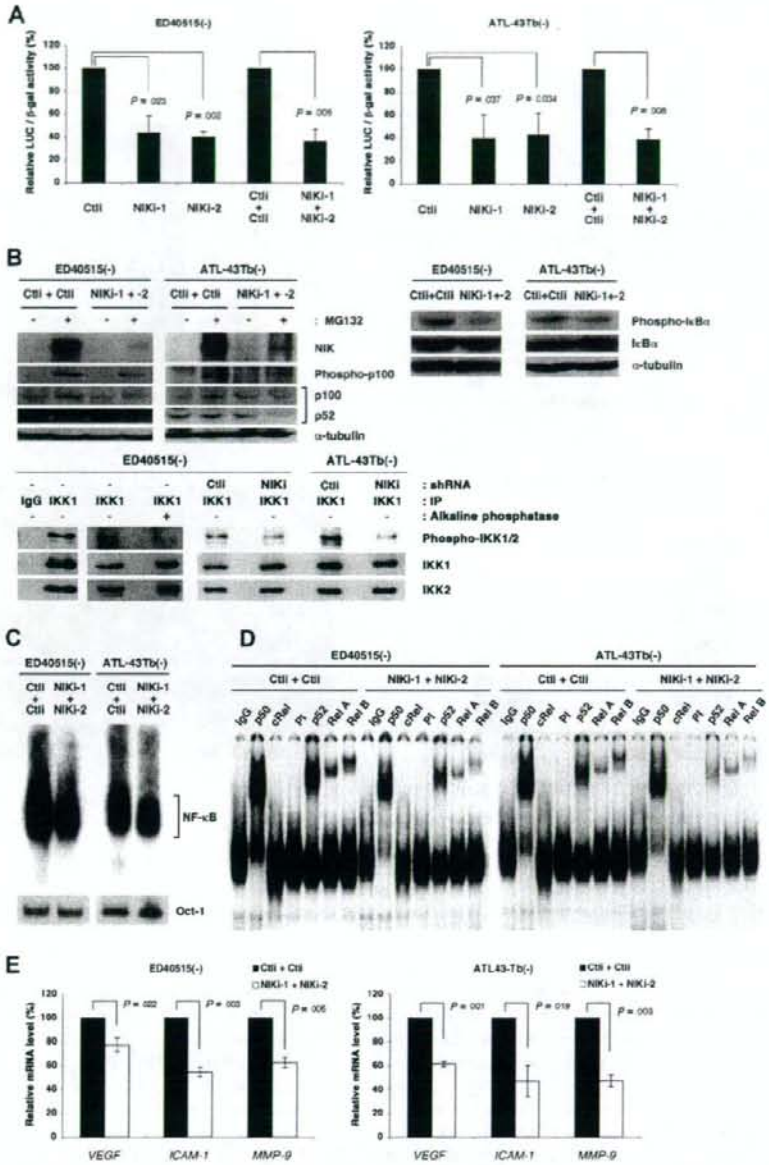

Figure 6. Depletion of NIK suppresses NF-κB-dependent transcription in ATL cells. (A) ED40515(−) and ATL-43Tb(−) cells were infected with lentiviral vectors expressing *Renilla luciferase* (Ctli) or *NIK*-specific shRNAs (NIKi-1 or NIKi-2). In parallel, ED40515(−) and ATL-43Tb(−) cells were infected with lentiviral vectors expressing Ctli or NIKi-1 shRNAs, and 24 hours later, these cells were super-infected with lentiviral vectors expressing Ctli or NIKi-2 shRNAs. Twenty-four hours after infection, cells were selected with puromycin for 2 days. Puromycin-resistant cells were then transfected with 2 μg of Igκ Cona-Luc and 2 μg EF1-LacZ. Luciferase (LUC) activity was determined 48 hours after transfection and normalized to β-gal activity. Relative luciferase activities, in comparison with control cells, 100 are shown. Data are expressed as mean plus or minus SD of 3 independent experiments. *P* values are versus control (Ctli). (B) Super-infected cells were treated with or without MG132 (20 μM) for 3 hours and subjected to SDS-PAGE and immunoblotting with anti-NIK (#4994), antiphosphorylated p100, or anti-α-tubulin antibodies. Whole-cell extracts (30 μg) from these cells were analyzed by SDS-PAGE and immunoblotting with antiphospho-IκBα, anti-IκBα, or anti-α-tubulin antibodies. Cytoplasmic extracts prepared from ED40515(−) cells infected or not with lentivirus were precleared and immunoprecipitation was performed, using anti-IKK1 monoclonal antibody or its isotype IgG (IgG). After 3 washes with TNT buffer, immune complexes were treated or not with Shrimp Alkaline Phosphatase (Takara Bio) and then subjected to SDS-PAGE and immunoblotting with antiphospho-IKK1/2, anti-IKK1, or anti-IKK2 antibodies. (C) A total of 5 μg of nuclear extracts prepared from lentivirus-infected cells shown in panel B were analyzed by EMSA, using oligonucleotides encoding the NF-κB–binding sequence or Oct-1–binding sequence as probes. (D) Nuclear extracts (5 μg) from lentivirus-infected cells shown in panel B were preincubated for 30 minutes with purified mouse IgG, anti-p50, anti-cRel antibody, preimmune (PI), anti-p50, anti-RelA or anti-RelB sera, and then subjected to EMSA with the NF-κB–specific probe. (E) Total RNAs from lentivirus-infected cells shown in panel B were examined by quantitative RT-PCR for *VEGF*, *ICAM-1*, and *MMP-9* mRNA levels. Each mRNA level was normalized to *18S RNA*. Relative mRNA levels, in comparison with control cells, 100 are shown. Data are expressed as mean plus or minus SD of 3 independent experiments. *P* values are versus control (Ctli + Ctli).

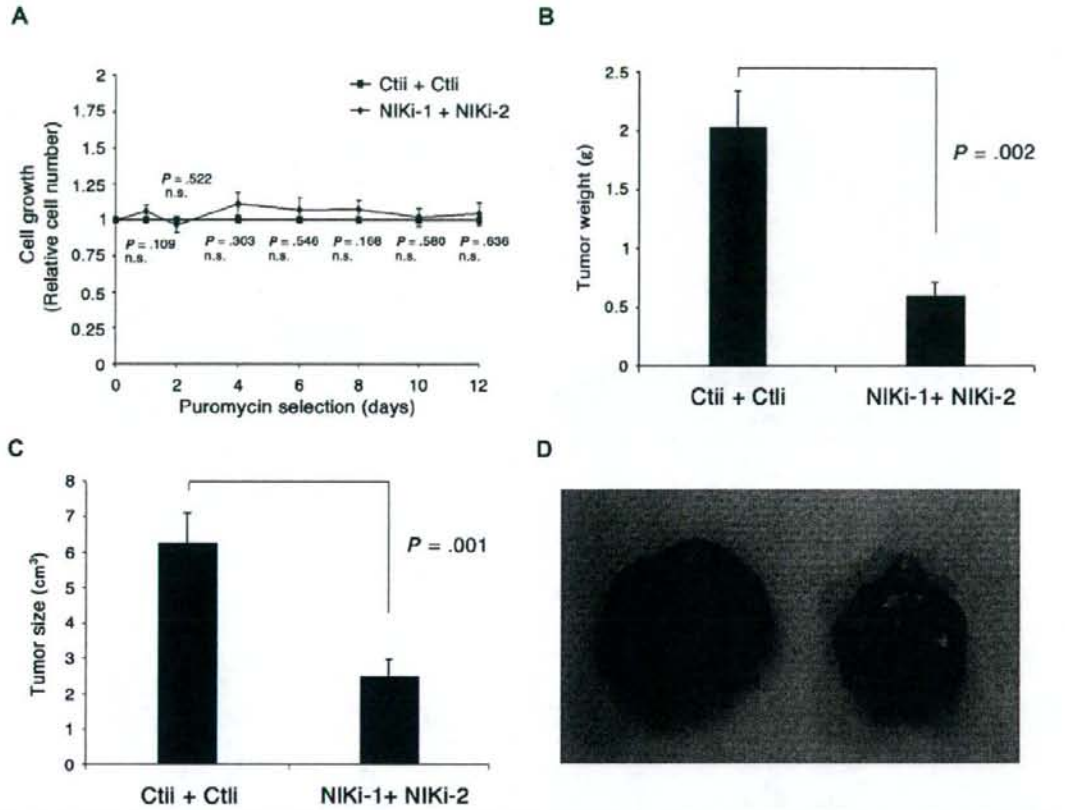

Figure 7. Depletion of NIK in ATL cells suppresses tumor formation in NOD-SCID/γc^{null} (NOG) mice. (A) Pools of ED40515(−) cells expressing Ctli or NIKi-1 and -2, shown in Figure 6B, C, D, and E, were analyzed for cell growth in vitro by the trypan blue staining method. Relative cell numbers, in comparison with control cells (arbitrarily set at 1), are shown. Data are expressed as mean plus or minus SD of 3 independent experiments. *P* values are vs control (Ctli + Ctli). n.s. indicates no significant difference. (B-D) NOG mice were inoculated subcutaneously in the postauricular region with the puromycin-resistant ED-40515(−) cells (5×10^6). Tumor formation in mice was evaluated 2 weeks after inoculation. Tumor weight (B) and size (C) relative to those of tumors formed in mice inoculated with ED40515(−) cells expressing Ctli are shown. (D) Photographs of tumors formed 2 weeks after cell inoculation. Each result was obtained from 5 different mice (means are shown [error bars]). *P* values are versus control (Ctli + Ctli).

loss of IKK activity after protein synthesis inhibition and the superinduction of IKK activity in the presence of MG132.[11] Moreover, RNA interference studies have also indicated that the deregulated NIK expression is the principal cause of constitutive NF-κB activation in ATL cells. In line with a previous report by Ramakrishnan et al, which showed that the induction of IκBα degradation by CD70, CD40 ligand, and BLyS/BAFF is dependent on the function of NIK,[18] we find in our present experiments that the stable expression of NIK induces IκBα phosphorylation and the formation of DNA binding complexes containing not only p50 and RelB, but also RelA both in wild-type and in NEMO-deficient rat fibroblasts. This indicates that NIK can stimulate the canonical pathway characterized by IκBα phosphorylation and RelA activation and that NIK does not require NEMO for it. Interestingly, the forced expression of SR-IκBα in these fibroblasts abolishes the transformed phenotype and suppresses constitutive NF-κB activity, with the p100 and p52 expression levels being diminished simultaneously, probably because p100 expression is largely dependent on NF-κB activity.[51] RelB expression is also known to be controlled by NF-κB,[52] suggesting that the noncanonical pathway of NF-κB activation does not work independently but rather coincides with NF-κB activation through the canonical pathway under stable conditions.

H-RS cells were also found to overexpress NIK, including its transcripts, in this study. Earlier reports have described 2 potential mechanisms of constitutive NF-κB activation in H-RS cells: persistent signaling from receptors that cause NF-κB activation, such as CD30, CD40, and RANK as well as a CD40-like molecule latent membrane protein 1 of the Epstein-Barr virus; and disruption of IκBα-dependent suppression resulting from the mutation of this gene.[32,48] The H-RS cell lines used in this study are Epstein-Barr virus-negative, and neither HDLM-2 nor L540 cells harbor mutations in their *IκB* genes. Indeed, CD30, CD40, and RANK were all found to be expressed in the H-RS cell lines used in this study, but we envisage that the aberrant expression of NIK is a distinct mechanism underlying the persistent NF-κB activation in these cells. It is partly because these TNF family receptor molecules, when stimulated or overexpressed transiently in cultured cells, elevate the NIK protein expression levels with a concomitant reduction in TRAF3 but do not increase *NIK* mRNA.[19,20]

Whereas the transient stimulation of a B-cell line with BAFF or anti-CD40 antibody stabilizes the NIK protein at the posttranslational level and does not up-regulate its mRNA expression,[20] NIK was observed to be constitutively overexpressed in ATL and H-RS cells at the pretranslational level. These differing mechanisms of NIK regulation may not be all that surprising, however, in light of the transient vs persistent nature of the activation of NF-κB. The barely detectable levels of steady-state NIK protein expression and its robust accumulation after proteasome inhibition in ATL and H-RS cells further suggest that the proteasome-dependent degradation of NIK occurs rapidly in tumor cells as in normal cells, although we cannot rule out the possibility that TNF family receptors known to be overexpressed in H-RS cells influence the stability of NIK to some extent. This point is currently very difficult to address because the protein amount of NIK in the absence of the proteasome inhibitor is quite limited. At least 3 mechanisms of pretranslational induction of NIK are plausible: the stabilization of *NIK* transcripts, transcriptional activation and/or amplification of the *NIK* gene. It should be noted that the stability of *NIK* mRNA in ATL cells was similar to that in control cells, suggesting that NIK expression is deregulated in ATL cells at the level of mRNA production. In this regard, we are currently analyzing the regulatory region of the *NIK* gene in normal and cancer cells.

We detected NIK in whole-cell lysates only when the cells themselves were treated with the proteasome inhibitor, MG132. It is possible that the expression of the NIK protein is tightly regulated under detectable levels in resting normal cells. However, in ATL and H-RS cells, enhanced NIK production, although still not detectable by simple immunoblotting, may be sufficient to cause its deregulated activity toward IKK. During the manuscript preparation, 2 reports demonstrated deregulated expression of NIK because of mutations in *TRAF3, CYLD*, or *NIK* itself in multiple myeloma cells.[16,17] In case of ATL cells, formation of a fusion protein after genomic rearrangement seems to be unlikely based on the apparently normal size of the protein. At present, the mechanism of overproduction of *NIK* mRNA in ATL cells remains to be determined, but the fluorescence in situ hybridization results suggest that aberrant NIK expression in ATL cells is not the result of genomic abnormalities, such as amplification or translocation.

Successful anticancer drug or gene therapies can be conducted in a number of ways, including the general administration of particular reagents that mechanistically work exclusively on cancer cells, or delivering conventional anticancer reagents specifically to cancer cells. The former strategy is likely to be more promising in the case of hematopoietic cancers. In this regard, NIK could be an attractive molecular target for ATL and Hodgkin lymphoma therapy, although the physiologic functions of NIK in human adults remain unknown. Suppressing high NF-κB activity levels by targeting NIK may also sensitize these cancer cells to commonly used anticancer agents.

Acknowledgments

The authors thank all of the ATL patients who donated blood samples for use in this study, Dr K. Yamaguchi and the Joint Study on Predisposing Factors of ATL Development for providing and analyzing sample blood, and the following researchers for donating invaluable reagents: Dr M. Maeda (Kyoto University, Kyoto, Japan) for the ED40515(−) and ATL-43Tb(−) cells, Dr D. Goeddel (Amgen, Thousand Oaks, CA) for *NIK* cDNAs, Dr N.R. Rice and Dr A. Israël (Institut Pasteur Paris, Paris, France) for p50, RelA, and RelB antisera, Dr T. Kitamura (University of Tokyo, Tokyo, Japan) for Plat-E cells, Dr I.S.Y. Chen (UCLA, Los Angeles, CA) for pHCMV-VSVG and pCMVΔR8.2 packaging plasmids, and Dr H. Miyoshi (RIKEN Tsukuba Institute, Tsukuba, Japan) for CS-CDF-CG-PRE plasmid. The authors also thank Dr G. Courtois (INSERM, Paris, France) and the members of the Department of Molecular Virology for helpful discussions.

This work was supported by research grants from the Ministry of Health and Labor Sciences (HIV/AIDS, H18-005) (Naoki Yamamoto) and from the Ministry of Education, Culture, Sports, Science and Technology of Japan (18390145; Naoki Yamamoto) and (17013029; S.Y.).

Authorship

Contribution: Y.S., T.S., and S.Y. designed the study; Y.S., Norio Yamamoto, H.S., V.J.M.B., Y.I., K.M., X.Q., I.I., J.I., and S.Y. carried out the research; M.Z.D. carried out the animal experiments; A.U. and T.W. collected and analyzed sample blood from ATL patients; T.M. contributed to lentiviral vector constructions; Y.S. and S.Y. analyzed the data; T.S., Naoki Yamamoto and S.Y. controlled the data; Y.S. and S.Y. wrote the paper; all authors checked the final version of the manuscript.

Conflict-of-interest disclosure: The authors declare no competing financial interests.

Correspondence: Shoji Yamaoka, Department of Molecular Virology, Graduate School of Medicine, Tokyo Medical and Dental University, 1-5-45, Yushima, Bunkyo-ku, Tokyo, 113-8510, Japan; e-mail: shojmmb@tmd.ac.jp.

References

1. Baldwin AS Jr. Series introduction: the transcription factor NF-kappaB and human disease. J Clin Invest. 2001;107:3-6.
2. Hayden MS, Ghosh S. Signaling to NF-kappaB. Genes Dev. 2004;18:2195-2224.
3. Xiao G, Rabson AB, Young W, Qing G, Qu Z. Alternative pathways of NF-kappaB activation: a double-edged sword in health and disease. Cytokine Growth Factor Rev. 2006;17:281-293.
4. Coope HJ, Atkinson PG, Huhse B, et al. CD40 regulates the processing of NF-kappaB2 p100 to p52. EMBO J. 2002;21:5375-5385.
5. Claudio E, Brown K, Park S, Wang H, Siebenlist U. BAFF-induced NEMO-independent processing of NF-kappa B2 in maturing B cells. Nat Immunol. 2002;3:958-965.
6. Karin M, Cao Y, Greten FR, Li ZW. NF-kappaB in cancer: from innocent bystander to major culprit. Nat Rev Cancer. 2002;2:301-310.
7. Jost PJ, Ruland J. Aberrant NF-{kappa}B signaling in lymphoma: mechanisms, consequences and therapeutic implications. Blood. 2006;109:2700-2707.
8. Ni H, Ergin M, Huang Q, et al. Analysis of expression of nuclear factor kappa B (NF-kappa B) in multiple myeloma: downregulation of NF-kappa B induces apoptosis. Br J Haematol. 2001;115:279-286.
9. Hironaka N, Mochida K, Mori N, Maeda M, Yamamoto N, Yamaoka S. Tax-independent constitutive IkappaB kinase activation in adult T-cell leukemia cells. Neoplasia. 2004;6:266-278.
10. Nonaka M, Horie R, Itoh K, Watanabe T, Yamamoto N, Yamaoka S. Aberrant NF-kappaB2/p52 expression in Hodgkin/Reed-Sternberg cells and CD30-transformed rat fibroblasts. Oncogene. 2005;24:3976-3986.
11. Miura H, Maeda M, Yamamoto N, Yamaoka S. Distinct IkappaB kinase regulation in adult T cell leukemia and HTLV-I-transformed cells. Exp Cell Res. 2005;308:29-40.
12. Dejardin E, Bonizzi G, Bellahcene A, Castronovo V, Merville MP, Bours V. Highly-expressed p100/p52 (NFKB2) sequesters other NF-kappa B-related proteins in the cytoplasm of human breast cancer cells. Oncogene. 1995;11:1835-1841.
13. Lessard L, Begin LR, Gleave ME, Mes-Masson AM, Saad F. Nuclear localization of nuclear factor-kappaB transcription factors in prostate cancer: an immunohistochemical study. Br J Cancer. 2005;93:1019-1023.
14. Chandler NM, Canete JJ, Callery MP. Increased

expression of NF-kappa B subunits in human pancreatic cancer cells. J Surg Res. 2004;118:9-14.

15. Bours V, Dejardin E, Goujon-Letawe F, Merville MP, Castronovo V. The NF-kappa B transcription factor and cancer: high expression of NF-kappa B- and I kappa B-related proteins in tumor cell lines. Biochem Pharmacol. 1994;47:145-149.
16. Annunziata CM, Davis RE, Demchenko Y, et al. Frequent engagement of the classical and alternative NF-kappaB pathways by diverse genetic abnormalities in multiple myeloma. Cancer Cell. 2007;12:115-130.
17. Keats JJ, Fonseca R, Chesi M, et al. Promiscuous mutations activate the noncanonical NF-kappaB pathway in multiple myeloma. Cancer Cell. 2007;12:131-144.
18. Ramakrishnan P, Wang W, Wallach D. Receptor-specific signaling for both the alternative and the canonical NF-kappaB activation pathways by NF-kappaB-inducing kinase. Immunity. 2004;21:477-489.
19. Liao G, Zhang M, Harhaj EW, Sun SC. Regulation of the NF-kappaB-inducing kinase by tumor necrosis factor receptor-associated factor 3-induced degradation. J Biol Chem. 2004;279:26243-26250.
20. Qing G, Qu Z, Xiao G. Stabilization of basally translated NF-kappaB-inducing kinase (NIK) protein functions as a molecular switch of processing of NF-kappaB2 p100. J Biol Chem. 2005;280:40578-40582.
21. Maeda M, Shimizu A, Ikuta K, et al. Origin of human T-lymphotrophic virus I-positive T cell lines in adult T cell leukemia: analysis of T cell receptor gene rearrangement. J Exp Med. 1985;162:2169-2174.
22. Yagi H, Nomura T, Nakamura K, et al. Crucial role of FOXP3 in the development and function of human CD25$^+$CD4$^+$ regulatory T cells. Int Immunol. 2004;16:1643-1656.
23. Sugamura K, Fujii M, Kannagi M, Sakitani M, Takeuchi M, Hinuma Y. Cell surface phenotypes and expression of viral antigens of various human cell lines carrying human T-cell leukemia virus. Int J Cancer. 1984;34:221-228.
24. Foley GE, Lazarus H, Farber S, Uzman BG, Boone BG, McCarthy RE. Continuous cultured human lymphoblasts from peripheral blood of a child with acute leukemia. Cancer. 1965;18:522-529.
25. Weiss A, Wiskocil RL, Stobo JD. The role of T3 surface molecules in the activation of human T cells: a two-stimulus requirement for IL 2 production reflects events occurring at pre-translational level. J Immunol. 1984;133:123-128.
26. Yamaoka S, Courtois G, Bessia C, et al. Complementation cloning of NEMO, a component of the IkappaB kinase complex essential for NF-kappaB activation. Cell. 1998;93:1231-1240.
27. Chinanonwait N, Miura H, Yamamoto N, Yamaoka S. A recessive mutant cell line with a constitutive IkappaB kinase activity. FEBS Lett. 2002;531:553-560.
28. Morita S, Kojima T, Kitamura T. Plat-E: an efficient and stable system for transient packaging of retroviruses. Gene Ther. 2000;7:1063-1066.
29. Yamaoka S, Inoue H, Sakurai M, et al. Constitutive activation of NF-kappa B is essential for transformation of rat fibroblasts by the human T-cell leukemia virus type I Tax protein. EMBO J. 1996;15:873-887.
30. Munoz E, Courtois G, Veschambre P, Jalinot P, Israël A. Tax induces nuclear translocation of NF-kappa B through dissociation of cytoplasmic complexes containing p105 or p100 but does not induce degradation of I kappa B alpha/MAD3. J Virol. 1994;68:8035-8044.
31. Dewan MZ, Terashima K, Taruishi M, et al. Rapid tumor formation of human T-cell leukemia virus type 1-infected cell lines in novel NOD-SCID/γc^{null} mice: suppression by an inhibitor against NF-κB. J Virol. 2003;77:5286-5294.
32. Krappmann D, Emmerich F, Kordes U, Scharschmidt E, Dorken B, Scheidereit C. Molecular mechanisms of constitutive NF-kappaB/Rel activation in Hodgkin/Reed-Sternberg cells. Oncogene. 1999;18:943-953.
33. Wood KM, Roff M, Hay RT. Defective IkappaBalpha in Hodgkin cell lines with constitutively active NF-kappaB. Oncogene. 1998;16:2131-2139.
34. Mori N, Fujii M, Ikeda S, et al. Constitutive activation of NF-kappaB in primary adult T-cell leukemia cells. Blood. 1999;93:2360-2368.
35. Yemelyanov A, Gasparian A, Lindholm P, et al. Effects of IKK inhibitor PS1145 on NF-kappaB function, proliferation, apoptosis and invasion activity in prostate carcinoma cells. Oncogene. 2006;25:387-398.
36. Farina AR, Tacconelli A, Vacca A, Maroder M, Gulino A, Mackay AR. Transcriptional up-regulation of matrix metalloproteinase-9 expression during spontaneous epithelial to neuroblast phenotype conversion by SK-N-SH neuroblastoma cells, involved in enhanced invasivity, depends upon GT-box and nuclear factor kappaB elements. Cell Growth Differ. 1999;10:353-367.
37. Collins T, Read MA, Neish AS, Whitley MZ, Thanos D, Maniatis T. Transcriptional regulation of endothelial cell adhesion molecules: NF-kappa B and cytokine-inducible enhancers. FASEB J. 1995;9:899-909.
38. El-Sabban ME, Merhi RA, Haidar HA, et al. Human T-cell lymphotropic virus type 1-transformed cells induce angiogenesis and establish functional gap junctions with endothelial cells. Blood. 2002;99:3383-3389.
39. Mori N, Sato H, Hayashibara T, et al. Human T-cell leukemia virus type I Tax transactivates the matrix metalloproteinase-9 gene: potential role in mediating adult T-cell leukemia invasiveness. Blood. 2002;99:1341-1349.
40. Hayashibara T, Yamada Y, Onimaru Y, et al. Matrix metalloproteinase-9 and vascular endothelial growth factor: a possible link in adult T-cell leukaemia cell invasion. Br J Haematol. 2002;116:94-102.
41. Fukudome K, Furuse M, Fukuhara N, Orita T, Hinuma Y. Strong induction of ICAM-1 in human T cells transformed by human T-cell leukemia virus type 1 and depression of ICAM-1 or LFA-1 in adult T-cell leukemia-derived cell lines. Int J Cancer. 1992;52:418-427.
42. Mori N, Yamada Y, Ikeda S, et al. Bay 11–7082 inhibits transcription factor NF-kappaB and induces apoptosis of HTLV-I-infected T-cell lines and primary adult T-cell leukemia cells. Blood. 2002;100:1828-1834.
43. Bargou RC, Emmerich F, Krappmann D, et al. Constitutive nuclear factor-kappaB-RelA activation is required for proliferation and survival of Hodgkin's disease tumor cells. J Clin Invest. 1997;100:2961-2969.
44. Yang J, Amiri KI, Burke JR, Schmid JA, Richmond A. BMS-345541 targets inhibitor of kappaB kinase and induces apoptosis in melanoma: involvement of nuclear factor kappaB and mitochondria pathways. Clin Cancer Res. 2006;12:950-960.
45. Gasparian AV, Yao YJ, Kowalczyk D, et al. The role of IKK in constitutive activation of NF-kappaB transcription factor in prostate carcinoma cells. J Cell Sci. 2002;115:141-151.
46. Wang CY, Cusack JC Jr, Liu R, Baldwin AS Jr. Control of inducible chemoresistance: enhanced anti-tumor therapy through increased apoptosis by inhibition of NF-kappaB. Nat Med. 1999;5:412-417.
47. Gilmore TD, Herscovitch M. Inhibitors of NF-kappaB signaling: 785 and counting. Oncogene. 2006;25:6887-6899.
48. Braun T, Carvalho G, Fabre C, Grosjean J, Fenaux P, Kroemer G. Targeting NF-kappaB in hematologic malignancies. Cell Death Differ. 2006;13:748-758.
49. Courtois G, Gilmore TD. Mutations in the NF-kappaB signaling pathway: implications for human disease. Oncogene. 2006;25:6831-6843.
50. Sun SC, Yamaoka S. Activation of NF-kappaB by HTLV-I and implications for cell transformation. Oncogene. 2005;24:5952-5964.
51. Liptay S, Schmid RM, Nabel EG, Nabel GJ. Transcriptional regulation of NF-kappa B2: evidence for kappa B-mediated positive and negative autoregulation. Mol Cell Biol. 1994;14:7695-7703.
52. Bren GD, Solan NJ, Miyoshi H, Pennington KN, Pobst LJ, Paya CV. Transcription of the RelB gene is regulated by NF-kappaB. Oncogene. 2001;20:7722-7733.